Ergodic Sum Capacity of Macrodiversity MIMO Systems in Flat Rayleigh Fading

Dushyantha A. Basnayaka, *Member, IEEE*, Peter J. Smith, *Senior Member, IEEE*, and Philippa A. Martin, *Senior Member, IEEE*

Abstract—The prospect of base station cooperation leading to joint combining at widely separated antennas has led to increased interest in macrodiversity systems, where both sources and receive antennas are geographically distributed. In this scenario, analytical investigation of channel capacity is extremely challenging for finite-size systems since the channel matrices have a very general form where each path may have a different power. Hence, in this paper, we consider the ergodic sum capacity of a macrodiversity multiple-input multiple-output system with arbitrary numbers of sources and receive antennas operating over Rayleigh fading channels. For this system, we compute the exact ergodic capacity for a system with at most two transmit antennas and a compact approximation for the general system, which is shown to be very accurate over a wide range of cases. Finally, we compare our results with previous asymptotic results and bounds. Results are verified by Monte Carlo simulations and the impact on capacity of various channel power profiles is investigated.

Index Terms—Capacity, CoMP, DAS, macrodiversity, MIMO, MIMO-MAC, network MIMO, Rayleigh fading, sum-rate.

I. INTRODUCTION

ITH the advent of network multiple-input multiple-output (MIMO) [1], base station (BS) collaboration [2], and cooperative MIMO [3], it is becoming more common to consider MIMO links where the receive array, transmit array, or both are widely separated. In these scenarios, individual antennas from a single effective array may be separated by a considerable distance. When both transmitter and receiver have distributed antennas, we refer to the link as a macrodiversity MIMO link. Fundamental analytical results for performance of such multiuser links are scarce, despite their growing importance in research [4]–[7] and standards where coordinated multipoint transmission is part of 3GPP LTE Advanced.

Manuscript received May 23, 2012; revised April 07, 2013; accepted May 10, 2013. Date of publication May 21, 2013; date of current version August 14, 2013. D. A. Basnayaka was supported by the University of Canterbury International Doctoral Scholarship.

D. A. Basnayaka was with the University of Canterbury, Christchurch 8140, New Zealand. He is now with the Institute for Digital Communication, University of Edinburgh, Edinburgh, EH8 9YL, U.K. (e-mail: d.basnayaka@ed.ac.uk).

P. J. Smith and P. A. Martin are with the Department of Electrical and Computer Engineering, University of Canterbury, Christchurch 8140, New Zealand (e-mail: p.smith@elec.canterbury.ac.nz; p.martin@elec.canterbury.ac.nz).

Communicated by A. Lozano, Associate Editor for Communications.

Color versions of one or more of the figures in this paper are available online at http://ieeexplore.ieee.org.

Digital Object Identifier 10.1109/TIT.2013.2264503

Some analytical progress in this area has been made recently in the performance analysis of linear combining for macrodiversity systems in Rayleigh fading [8], [9]. However, work on this specific capacity problem for a finite-size system in a macrodiversity layout is very limited. There are a large number of related works, but these tend to consider different channels, simplified assumptions, and asymptotic approaches. For example, similar work includes the capacity analysis of Rayleigh channels with a two-sided Kronecker correlation structure [10]. However, the Kronecker structure is too much restrictive for a macrodiversity layout and such results cannot be leveraged here. Work has been done on system capacity for particular cellular structures, including Wyner's circular cellular array model [6] and the infinite linear cell-array model [7]. There is a large body of research on distributed antenna systems where a Gaussian assumption is used for modeling interference plus noise for simplifying analytical derivations [11]–[13]. In some other work, crude approximations are used, which are sensible, but appear insufficient to model the complex interdependence of desired and interfering sources [14]. On another front, an asymptotic large random matrix approach is employed to derive a deterministic equivalent to the ergodic sum capacity in [15] and [16]. Similarly, an asymptotic approach is used to study cellular systems with multiple correlated BSs and user antennas in [17] and [18]. A comparative study on uplink sum capacity with colocated and distributed antennas can be found in [19] and [20]. Of particular relevance to the current work is the asymptotic analysis given in [21]. The exact asymptotic capacity is derived which applies to general independent channel matrices and not just the Rayleigh case in [21]. These powerful results also provide accurate approximations to finite system capacity. In Section VII, we show that the new approximations developed here make further improvements on the accuracy of these results.

Despite these contributions, the general macrodiversity model appears difficult to handle for finite-size systems. The analytical difficulties are caused by the geographical separation of the antennas which results in different entries of the channel matrix having different powers with an arbitrary pattern. Also, these powers can vary enormously when shadowing and path loss are considered. Note that this type of channel model also occurs in the work of [22]. When the receive antennas are colocated, classical models and the use of a Kronecker correlation matrix lead to a Wishart form. This allow extensive results in multivariate statistics to be leveraged and performance analysis is well advanced [23], [24]. In contrast, the macrodiversity case violates the Wishart assumptions making the analytical work extremely difficult. The analytical complexity is clearly

evident even in the simplest case of a dual source scenario in Section IV

In this paper, we consider a macrodiversity MIMO multiple access channel (MIMO-MAC) where all sources and receive antennas are widely separated and all links experience independent Rayleigh fading. For this system, we consider the ergodic sum capacity, under the assumption of no channel state information (CSI) at the transmitters. For two sources, we derive the exact ergodic sum capacity. The result is given in closed form, but the details are complicated, and for more than two sources, it would appear that an exact approach is too complex to be useful. Hence, we develop an approximation and compare the accuracy of this approximation to the asymptotic results in [21] and the bound in [27]. Furthermore, we use the bound in [27] to gain insight into capacity behavior and its relationship with the channel powers. In [25], we presented a preliminary study of this problem, which focused on the approximation for the general case. In this paper, we have extended the conference version to include the exact two source results, correlated channels, full mathematical details (see Section III), a motivation for the approximate analysis (see Appendix B), and a much wider range of scenarios, power profiles, and discussion in the results section.

Note that the methodology developed is for the case of arbitrary powers for the entries in the channel matrix. There is no restriction due to particular cellular structures. Hence, the results and techniques may also have applications in multivariate statistics.

The rest of this paper is laid out as follows. Section II describes the system model and Section III gives some mathematical preliminaries required in the analysis. Section IV provides an exact analysis for the case of two source antennas. Sections V and VI consider the case of arbitrary numbers of sources and develop accurate approximations of capacity. Results and conclusions appear in Sections VII and VIII, respectively.

II. SYSTEM MODEL

Consider a MIMO-MAC link with M BSs and W users operating over a Rayleigh channel, where BS i has n_{R_i} receive antennas and user i has n_i antennas. The total number of receive antennas is denoted $n_R = \sum_{i=1}^M n_{R_i}$ and the total number of transmit antennas is denoted $N = \sum_{i=1}^W n_i$. An example of such a system is shown in Fig. 1, where three BSs are linked by a backhaul processing unit and communicate with multiple, mobile users. All channels are considered to be independent since the correlated channel scenario can be transformed into the independent case as shown in Section II-A. The system equation is given by

$$r = Hs + n. (1)$$

where \mathbf{r} is the $C^{n_R \times 1}$ receive vector, \mathbf{s} is the combined $C^{N \times 1}$ transmitted vector from the W users, \mathbf{n} is an additive white Gaussian noise vector, $\mathbf{n} \sim \mathcal{CN}\left(\mathbf{0}, \sigma^2 \mathbf{I}\right)$, and $\mathbf{H} \in C^{n_R \times N}$ is the composite channel matrix containing the W channel matrices from the W users. The ergodic sum capacity of the link

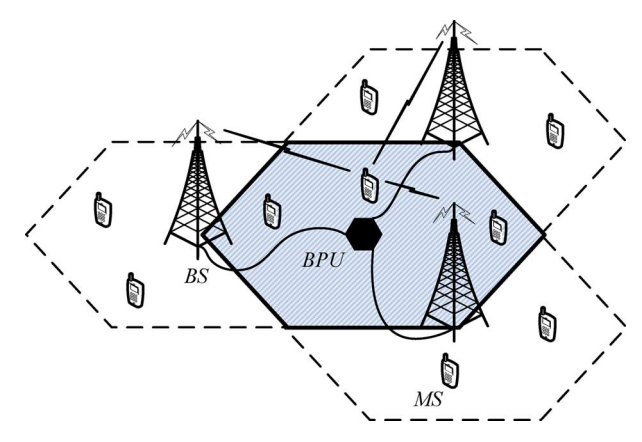


Fig. 1. Network MIMO system with a three-sector cluster. To reduce the clutter, only paths from a single source are shown.

depends on the availability of CSI at the transmitter side. In particular, if no CSI at the transmitter is assumed, the corresponding ergodic sum capacity is [3, p. 57]

$$E\{C\} = E\left\{\log_2\left|\boldsymbol{I} + \frac{1}{\sigma^2}\boldsymbol{H}\boldsymbol{H}^H\right|\right\},\tag{2}$$

where $E\left\{|s_i|^2\right\}=1,\ i=1,2,\ldots,N,$ is the power of each transmitted symbol. It is convenient to label each column of \boldsymbol{H} as $\boldsymbol{h}_i,\ i=1,2,\ldots,N,$ so that $\boldsymbol{H}=(\boldsymbol{h}_1,\boldsymbol{h}_2,\ldots,\boldsymbol{h}_N).$ The covariance matrix of \boldsymbol{h}_k is defined by $\boldsymbol{P}_k=E\left\{\boldsymbol{h}_k\boldsymbol{h}_k^H\right\}$ and $\boldsymbol{P}_k=\operatorname{diag}\left(P_{1k},P_{2k},\ldots,P_{n_Rk}\right).$ Hence, the (i,k)-th element of \boldsymbol{H} is $\mathcal{CN}\left(0,P_{ik}\right).$ Using this notation, we can also express \boldsymbol{h}_k as $\boldsymbol{h}_k=\boldsymbol{P}_k^{\frac{1}{2}}\boldsymbol{u}_k$, where $\boldsymbol{u}_k\sim\mathcal{CN}\left(\boldsymbol{0},\boldsymbol{I}\right).$ Note that, for convenience, all the power information is contained in the \boldsymbol{P}_k matrices so that there is no normalization of the channel and, in (2), the scaling factor in the capacity equation is simply $1/\sigma^2.$

A. Correlated Channels

Consider the general scenario where sources and/or BSs have multiple colocated antennas for transmission and reception. Here, spatial correlation may be present due to the colocated antennas [21], [26]. If a Kronecker correlation model is assumed, then the composite channel matrix is given by

$$oldsymbol{H} = egin{pmatrix} oldsymbol{R}_{r1}^{rac{1}{2}} & oldsymbol{0} \ dots \ oldsymbol{0} \ oldsymbol{0} \ oldsymbol{R}_{rM} \end{pmatrix} egin{pmatrix} oldsymbol{H}_{w,11} \dots oldsymbol{H}_{w,1W} \ dots \ oldsymbol{0} \ oldsymbo$$

where the $\mathcal{C}^{n_{R_k} \times n_i}$ matrix, $\boldsymbol{H}_{w,ik}$, has i.i.d. elements since all the channel powers from user k to BS i are the same. The matrix \boldsymbol{R}_{ri} is the receive correlation matrix at BS i and the matrix \boldsymbol{R}_{tk} is the transmit correlation matrix at source k as defined in [26]. Using the spectral decompositions, $\boldsymbol{R}_{ri} = \boldsymbol{\Phi}_{ri}\boldsymbol{\Lambda}_{ri}\boldsymbol{\Phi}_{ri}^H$ and $\boldsymbol{R}_{tk} = \boldsymbol{\Phi}_{tk}\boldsymbol{\Lambda}_{tk}\boldsymbol{\Phi}_{tk}^H$, and substituting (3) into (2), it is easily shown that the capacity with the channel in (3) is statistically identical to the capacity with channel

$$\boldsymbol{H} = \begin{pmatrix} \boldsymbol{\Lambda}_{r1}^{\frac{1}{2}} & \boldsymbol{0} \\ & \ddots & \\ \boldsymbol{0} & \boldsymbol{\Lambda}_{rM}^{\frac{1}{2}} \end{pmatrix} \begin{pmatrix} \boldsymbol{H}_{w,11} \dots \boldsymbol{H}_{w,1W} \\ \vdots & \ddots & \vdots \\ \boldsymbol{H}_{w,M1} \dots \boldsymbol{H}_{w,MW} \end{pmatrix} \begin{pmatrix} \boldsymbol{\Lambda}_{t1}^{\frac{1}{2}} & \boldsymbol{0} \\ & \ddots & \\ \boldsymbol{0} & \boldsymbol{\Lambda}_{tW}^{\frac{1}{2}} \end{pmatrix}.$$
(4)

Denoting (4) by $\boldsymbol{H} = \boldsymbol{\Lambda}_r^{\frac{1}{2}} \boldsymbol{H}_w \boldsymbol{\Lambda}_t^{\frac{1}{2}}$, we see that correlation is equivalent to a scaling of the channel by the relevant eigenvalues in $\boldsymbol{\Lambda}_r$ and $\boldsymbol{\Lambda}_t$. In particular, the (u,v) th element of \boldsymbol{H} has power $\boldsymbol{\Lambda}_{r,uu} \boldsymbol{\Lambda}_{t,vv} \tilde{P}_{uv}$, where \tilde{P}_{uv} is the single link power from transmit antenna v to receive antenna u. Hence, correlation can be handled by the same methodology developed in Sections IV–VI, with suitably scaled power values.

III. PRELIMINARIES

In this section, we state some useful results which will be used extensively throughout the paper.

Let $\mathbf{A} = (a_{ik})$ be an $m \times n$ rectangular matrix over the commutative ring, $m \leq n$. The permanent of \mathbf{A} , written $\operatorname{Perm}(\mathbf{A})$, is defined by

$$\operatorname{Perm}(\mathbf{A}) = \sum_{\sigma} a_{1,\sigma_1} a_{2,\sigma_2} \dots a_{m,\sigma_m}, \tag{5}$$

where the summation extends over all one-to-one functions from $\{1,\ldots,m\}$ to $\{1,\ldots,n\}$. The sequence $(a_{1,\sigma_1}a_{2,\sigma_2}\ldots a_{m,\sigma_m})$ is called a diagonal of \boldsymbol{A} , and the product $a_{1,\sigma_1}a_{2,\sigma_2}\ldots a_{m,\sigma_m}$ is a diagonal product of \boldsymbol{A} . Thus, the permanent of \boldsymbol{A} is the sum of all diagonal products of \boldsymbol{A} .

Lemma 1 [27]: Let X be an $m \times n$ random matrix with independent zero mean Gaussian distributed elements with,

$$\mathbf{A} = E\left\{ \mathbf{X} \circ \bar{\mathbf{X}} \right\} \triangleq \begin{pmatrix} E\left\{ |X_{11}|^2 \right\} & \dots & E\left\{ |X_{1n}|^2 \right\} \\ E\left\{ |X_{21}|^2 \right\} & \dots & E\left\{ |X_{2n}|^2 \right\} \\ \dots & \dots & \dots \\ E\left\{ |X_{m1}|^2 \right\} & \dots & E\left\{ |X_{mn}|^2 \right\} \end{pmatrix},$$
(6)

where \circ represents the Hadamard product. The matrix \bar{X} is the elementwise conjugate of X. With this notation, the following identity holds:

$$E\{|\mathbf{X}^{H}\mathbf{X}|\} = \begin{cases} \operatorname{perm}(\mathbf{A}) & m = n \\ \operatorname{Perm}(\mathbf{A}) & m > n, \end{cases}$$

where perm(.) and Perm (.) are the permanent of a square matrix and rectangular matrix, respectively, as defined in [28].

Corollary 1: Let X be an $m \times n$ random matrix with $E\{X \circ \bar{X}\} = A$, where A is an $m \times n$ deterministic matrix and m > n. If the $m \times m$ deterministic matrix Σ is diagonal, then the following identity holds:

$$E\left\{\left|\boldsymbol{X}^{H}\boldsymbol{\Sigma}\boldsymbol{X}\right|\right\} = \operatorname{Perm}\left(\boldsymbol{\Sigma}\boldsymbol{A}\right).$$
 (7)

Proof: The result follows directly from Lemma 1 and the fact that $\Sigma^{\frac{1}{2}} \circ \Sigma^{\frac{1}{2}} = \Sigma$ for any diagonal matrix.

Next, we give a definition for the elementary symmetric function (esf) of degree k in n variables, X_1, X_2, \ldots, X_n [29]. Let $e_k(X_1, X_2, \ldots, X_n)$ be the kth degree esf; then

$$e_k(X_1, X_2, \dots, X_n) = \sum_{1 \le l_1 < l_2 < \dots < l_k \le n} X_{l_1} \dots X_{l_k}.$$
 (8)

¹Arbitrary fixed transmit power control techniques can also be handled in the same way as for the correlated scenario.

It is apparent from (8) that $e_0(X_1, X_2, ..., X_n) = 1$ and $e_n(X_1, X_2, ..., X_n) = X_1 X_2 ... X_n$. In general, the esf of degree k in n variables, for any $k \le n$, is formed by adding together all distinct products of k distinct variables.

Lemma 2 [29]: let X be an $n \times n$ complex symmetric positive-definite matrix with eigenvalues $\lambda_1, \ldots, \lambda_n$. Then, the following identity holds:

$$e_k(\lambda_1, \lambda_2, \dots, \lambda_n) = \operatorname{Tr}_k(\boldsymbol{X}),$$
 (9)

where

$$\operatorname{Tr}_{k}(\boldsymbol{X}) = \begin{cases} \sum_{\sigma} \left| \boldsymbol{X}_{\sigma_{k,n}} \right| & 1 \leq k \leq n \\ 1 & k = 0 \\ 0 & k > n, \end{cases}$$
 (10)

and $\sigma_{k,n}$ is an ordered subset of $\{n\} = \{1, \ldots, n\}$ of length k and the summation is over all such subsets. $\boldsymbol{X}_{\sigma_{k,n}}$ denotes the principal submatrix of \boldsymbol{X} formed by taking only the rows and columns indexed by $\sigma_{k,n}$.

In general, $X_{\sigma_{\ell,n}}^{\mu_{\ell,n}}$ denotes the submatrix of X formed by taking only the rows and columns indexed by $\sigma_{\ell,n}$ and $\mu_{\ell,n}$, respectively, where $\sigma_{\ell,n}$ and $\mu_{\ell,n}$ are length ℓ subsets of $\{1,2,\ldots,n\}$. If either $\sigma_{\ell,n}$ or $\mu_{\ell,n}$ contains the complete set (i.e., $\sigma_{\ell,n}=\{1,2,\ldots,n\}$) or $\mu_{\ell,n}=\{1,2,\ldots,n\}$), the corresponding subscript/superscript may be dropped. When $\sigma_{\ell,n}=\mu_{\ell,n}$, only one subscript/superscript may be shown for brevity.

Next, we present three axiomatic identities for permanents which are required in Section V.

1) Axiom 1: For an empty matrix, A,

$$Perm(\mathbf{A}) = 1. \tag{11}$$

2) Axiom 2: Let \mathbf{A} be an arbitrary $m \times n$ matrix, then

$$\sum_{\sigma} \operatorname{Perm} \left((\boldsymbol{A})^{\sigma_{0,n}} \right) = \sum_{\sigma} \operatorname{Perm} \left((\boldsymbol{A})_{\sigma_{0,m}} \right) = 1. \quad (12)$$

3) Axiom 3: Let A be an arbitrary $m \times n$ matrix, then

$$\sum_{\sigma} \operatorname{Perm}\left((\boldsymbol{A})_{\sigma_{k,m}} \right) = \sum_{\sigma} \operatorname{Perm}\left((\boldsymbol{A})^{\sigma_{k,n}} \right). \tag{13}$$

IV. EXACT SMALL SYSTEM ANALYSIS

In this section, we derive the exact ergodic sum capacity in (2) for the N=2 case. This corresponds to two single-antenna users or a single user with two distributed antennas. Here, the channel matrix becomes $\boldsymbol{H}=(\boldsymbol{h}_1,\boldsymbol{h}_2)$ and it is straightforward to write (2) as

$$E\{C\} \ln 2 = E\left\{ \ln \left| \boldsymbol{I} + \frac{1}{\sigma^2} \boldsymbol{h}_1 \boldsymbol{h}_1^H \right| \right\}$$

$$+ E\left\{ \ln \left| \boldsymbol{I} + \frac{1}{\sigma^2} \left(\boldsymbol{I} + \frac{1}{\sigma^2} \boldsymbol{h}_1 \boldsymbol{h}_1^H \right)^{-1} \boldsymbol{h}_2 \boldsymbol{h}_2^H \right| \right\}$$

$$\triangleq C_1 + C_2. \tag{14}$$

Both C_1 and C_2 can be expressed as scalars [30], [31, p. 48], so the capacity analysis simply requires

$$C_1 = E\left\{\ln\left(1 + \frac{1}{\sigma^2}\boldsymbol{h}_1^H\boldsymbol{h}_1\right)\right\},\tag{15}$$

$$C_2 = E \left\{ \ln \left(1 + \frac{1}{\sigma^2} \boldsymbol{h}_2^H \left(\boldsymbol{I} + \frac{1}{\sigma^2} \boldsymbol{h}_1 \boldsymbol{h}_1^H \right)^{-1} \boldsymbol{h}_2 \right) \right\}. (16)$$

In order to facilitate our analysis, it is useful to avoid the logarithm representations in (15) and (16). We exchange logarithms for exponentials as follows. First, we note the identity

$$\frac{1}{a} = \int_0^\infty e^{-at} dt, \quad \text{for} \quad a > 0.$$
 (17)

Now (17) can be used to find $\ln a$ as follows:

$$\frac{\partial \ln a}{\partial a} = \int_0^\infty e^{-at} dt,\tag{18}$$

$$\int_0^{\ln a} d\ln a = \int_1^a \int_0^\infty e^{-at} dt da, \tag{19}$$

$$\ln a = \int_0^\infty \frac{e^{-t} - e^{-at}}{t} dt. \tag{20}$$

This manipulation is useful because there are many results which can be applied to exponentials of quadratic forms, whereas few results exist for logarithms. As an example, using (20) in (15) gives

$$C_1 = E\left\{ \int_0^\infty \frac{e^{-t} - e^{-\left(1 + \frac{1}{\sigma^2} \mathbf{h}_1^H \mathbf{h}_1\right)t}}{t} dt \right\}. \tag{21}$$

Note that $a=1+\frac{1}{\sigma^2}\boldsymbol{h}_1^H\boldsymbol{h}_1$ has been used in (20). Since $a\geq 1$, it follows that the integrand in (21) is nonnegative. Also, the expected value, C_1 , is clearly finite, and so, by Fubini's theorem, the order of expectation and integration in (21) may be interchanged. Using the Gaussian integral identity [9], the expectation in (21) can be computed to give

$$C_1 = \int_0^\infty \frac{e^{-t}}{t} - \frac{e^{-t}}{t|\mathbf{\Sigma}_1|} dt, \tag{22}$$

where $\Sigma_1 = I + \frac{t}{\sigma^2} P_1$. Hence, the log-exponential conversion in (20) leads to a manageable integral for C_1 . Note that there are many alternative routes to derive C_1 . Similar quadratic forms are common in communication problems and related work can be found in [32] and [33]. This particular approach is useful here as it applies to both C_1 and C_2 . It is also useful in Section V where more than two source antennas are considered. Using the same approach and applying (20) in (16) gives

 $C_{2} = E \left\{ \int_{0}^{\infty} \frac{e^{-t}}{t} - \frac{e^{-t - \frac{t}{\sigma^{2}} \mathbf{h}_{2}^{H} (\mathbf{I} + \frac{1}{\sigma^{2}} \mathbf{h}_{1} \mathbf{h}_{1}^{H})^{-1} \mathbf{h}_{2}}}{t} dt \right\}. (23)$

The expectation in (23) has to be calculated in two stages. First, the expectation over h_2 can be solved using the Gaussian integral identity [9] and, with some simplifications, we arrive at

$$C_2 = \int_0^\infty \frac{e^{-t}}{t} - E_{\mathbf{h}_1} \left\{ \frac{e^{-t} \left(\sigma^2 + \mathbf{h}_1^H \mathbf{h}_1\right)}{t \left|\mathbf{\Sigma}_2\right| \left(\sigma^2 + \mathbf{h}_1^H \mathbf{\Sigma}_2^{-1} \mathbf{h}_1\right)} \right\} dt, \quad (24)$$

where $\Sigma_2 = I + \frac{t}{\sigma^2} P_2$. Interchange of the expectation and integral in (24) follows from the same arguments used for C_1 . Equation (24) can be further simplified to give

$$C_{2} = \int_{0}^{\infty} \frac{e^{-t}}{t} - \frac{e^{-t}}{t |\mathbf{\Sigma}_{2}|} dt$$
$$- E_{\mathbf{h}_{1}} \left\{ \frac{1}{\sigma^{2}} \int_{0}^{\infty} \frac{e^{-t} \mathbf{h}_{1}^{H} \mathbf{P}_{2} \mathbf{\Sigma}_{2}^{-1} \mathbf{h}_{1}}{t |\mathbf{\Sigma}_{2}| \left(\sigma^{2} + \mathbf{h}_{1}^{H} \mathbf{\Sigma}_{2}^{-1} \mathbf{h}_{1}\right)} dt \right\}. (25)$$

Defining the third term in (25) as I_b , the ergodic sum capacity, $E\left(C\right)=C_1+C_2$, becomes

$$E\{C\} = \frac{1}{\ln 2} \left\{ \sum_{k=1}^{2} I_{a_k} - I_b \right\},\tag{26}$$

where

$$I_{a_k} = \int_0^\infty \left(\frac{e^{-t}}{t} - \frac{e^{-t}}{t |\mathbf{\Sigma}_k|} \right) dt. \tag{27}$$

Substituting for Σ_k into (27) and expanding $(t | \Sigma_k|)^{-1}$ gives

$$I_{a_k} = \sum_{i=1}^{n_R} \eta_{ik} \int_0^\infty \frac{e^{-t}}{t + \frac{\sigma^2}{P_{ik}}} dt,$$
 (28)

where

$$\eta_{ik} = \frac{P_{ik}^{n_R - 1}}{\prod_{l \neq i}^{n_R} (P_{ik} - P_{lk})}.$$
 (29)

Note that the first e^{-t}/t term in (27) cancels out with one of the terms in the partial fraction expansion leaving only the linear terms shown in the denominator of (28). The integrals in (28) can be solved in closed form [34] to give

$$I_{a_k} = \sum_{i=1}^{n_R} \eta_{ik} e^{\frac{\sigma^2}{P_{ik}}} E_1\left(\frac{\sigma^2}{P_{ik}}\right).$$
 (30)

In order to compute I_b , we use [9, Lemma 1] to give

$$I_b = -\int_0^\infty \int_0^\infty \frac{e^{-t}}{|\mathbf{\Sigma}_2|} \left. \frac{\partial E\left\{ e^{-\theta_1 z_1 - \theta_2 z_2} \right\}}{\partial \theta_1} \right|_{\theta_1 = 0} d\theta_2 dt, \quad (31)$$

where $z_1 = \boldsymbol{h}_1^H \boldsymbol{P}_2 \boldsymbol{\Sigma}_2^{-1} \boldsymbol{h}_1$ and $z_2 = \sigma^2 + \boldsymbol{h}_1^H \boldsymbol{\Sigma}_2^{-1} \boldsymbol{h}_1$. The expectation in (31) can be solved as in [9], and with some manipulations, we arrive at

$$I_{b} = -\int_{0}^{\infty} \int_{0}^{\infty} \frac{\partial}{\partial \theta_{1}} \left[\frac{e^{-\sigma^{2}t - \sigma^{2}\theta_{2}}}{|\mathbf{I} + t\mathbf{P}_{2} + \theta_{1}\mathbf{P}_{1}\mathbf{P}_{2} + \theta_{2}\mathbf{P}_{1}|} \right]_{\theta_{1} = 0} d\theta_{2} dt.$$
(32)

In Appendix A, I_b in (32) is calculated in closed form and the final result is given by

$$I_{b} = -\frac{1}{|\mathbf{P}_{1}\mathbf{P}_{2}|} \left\{ \sum_{i=1}^{n_{R}} \sum_{k \neq i}^{n_{R}} \sum_{l \neq i,k}^{n_{R}} \frac{\xi_{ikl} \left(\tilde{M}_{b_{ikl}} - \tilde{N}_{b_{ikl}} \right)}{J_{i}} \right\},$$
(33)

where $\tilde{M}_{b_{ikl}}$, $\tilde{N}_{b_{ikl}}$, J_i , and ξ_{ikl} are given in (90), (91), (68), and (78), respectively. Then, the final result becomes

$$E\{C\} = \frac{1}{\ln 2} \left\{ \sum_{k=1}^{2} \sum_{i=1}^{n_R} \eta_{ik} e^{\frac{\sigma^2}{\tilde{P}_{ik}}} E_1 \left(\frac{\sigma^2}{P_{ik}} \right) + \frac{1}{|\mathbf{P}_1 \mathbf{P}_2|} \left[\sum_{i=1}^{n_R} \sum_{k \neq i}^{n_R} \sum_{l \neq i,k}^{n_R} \frac{\xi_{ikl} \left(\tilde{M}_{b_{ikl}} - \tilde{N}_{b_{ikl}} \right)}{J_i} \right] \right\}.$$
(34)

Note that the final result is a complex function of the channel powers which also appear inside the exponential integral. Hence, further optimization of system parameters, such as transmit powers, will be difficult.

V. APPROXIMATE GENERAL ANALYSIS

In this section, we present an approximate ergodic sum rate capacity analysis for the case where $n_R \geq N > 2$. Extending this to $N \geq n_R$ is a simple extension of the current analysis. We use the following notation for the channel matrix:

$$\boldsymbol{H} = \left(\tilde{\boldsymbol{H}}_{N}, \boldsymbol{h}_{N}\right) \tag{35a}$$

$$= \left(\tilde{\boldsymbol{H}}_{N-1}, \boldsymbol{h}_{N-1}, \boldsymbol{h}_{N}\right) \tag{35b}$$

$$= \left(\tilde{\boldsymbol{H}}_{k}, \boldsymbol{h}_{k} \dots, \boldsymbol{h}_{N-1}, \boldsymbol{h}_{N}\right) \tag{35c}$$

$$= \vdots$$

$$= (\boldsymbol{h}_1, \boldsymbol{h}_2, \dots, \boldsymbol{h}_N), \qquad (35d)$$

where the $n_R \times (k-1)$ matrix, $\tilde{\boldsymbol{H}}_k$, comprises the k-1 columns to the left of \boldsymbol{h}_k in \boldsymbol{H} . Using the same representation as in (14), the ergodic sum capacity is defined [3] as

$$E\{C\} \ln 2 \triangleq \sum_{k=1}^{N} C_k, \tag{36}$$

where

$$C_{k} = E \left\{ \ln \left| \boldsymbol{I} + \frac{1}{\sigma^{2}} \left(\boldsymbol{I} + \frac{1}{\sigma^{2}} \tilde{\boldsymbol{H}}_{k} \tilde{\boldsymbol{H}}_{k}^{H} \right)^{-1} \boldsymbol{h}_{k} \boldsymbol{h}_{k}^{H} \right| \right\}$$
(37)
$$= E \left\{ \ln \left(1 + \frac{1}{\sigma^{2}} \boldsymbol{h}_{k}^{H} \left(\boldsymbol{I} + \frac{1}{\sigma^{2}} \tilde{\boldsymbol{H}}_{k} \tilde{\boldsymbol{H}}_{k}^{H} \right)^{-1} \boldsymbol{h}_{k} \right) \right\}.$$
(38)

Applying (20) to (38) gives

$$C_{k} = \int_{0}^{\infty} \frac{e^{-t}}{t} - E \left\{ \frac{e^{-t} \left| \sigma^{2} \mathbf{I} + \tilde{\mathbf{H}}_{k}^{H} \tilde{\mathbf{H}}_{k} \right|}{t \left| \mathbf{\Sigma}_{k} \right| \left| \sigma^{2} \mathbf{I} + \tilde{\mathbf{H}}_{k}^{H} \mathbf{\Sigma}_{k}^{-1} \tilde{\mathbf{H}}_{k} \right|} \right\} dt, \quad (39)$$

where $\Sigma_k = I + \frac{t}{\sigma^2} P_k$. In order to calculate the second term in (39), the following expectation needs to be calculated:

$$\tilde{I}_{k}\left(t\right) = \frac{1}{\left|\boldsymbol{\Sigma}_{k}\right|} E\left\{ \frac{\left|\sigma^{2}\boldsymbol{I} + \tilde{\boldsymbol{H}}_{k}^{H} \tilde{\boldsymbol{H}}_{k}\right|}{\left|\sigma^{2}\boldsymbol{I} + \tilde{\boldsymbol{H}}_{k}^{H} \boldsymbol{\Sigma}_{k}^{-1} \tilde{\boldsymbol{H}}_{k}\right|} \right\}.$$
 (40)

Exact analysis of $\tilde{I}_k(t)$ is cumbersome, and even the N=2 case [see the I_b calculation in (32)] is complicated. Hence, we employ a Laplace type approximation [35], so that $\tilde{I}_k(t)$ can be approximated by

$$\tilde{I}_{k}\left(t\right) \simeq \frac{1}{\left|\boldsymbol{\Sigma}_{k}\right|} \frac{E\left\{\left|\sigma^{2}\boldsymbol{I} + \tilde{\boldsymbol{H}}_{k}^{H}\tilde{\boldsymbol{H}}_{k}\right|\right\}}{E\left\{\left|\sigma^{2}\boldsymbol{I} + \tilde{\boldsymbol{H}}_{k}^{H}\boldsymbol{\Sigma}_{k}^{-1}\tilde{\boldsymbol{H}}_{k}\right|\right\}}.$$
(41)

Note that the Laplace approximation is better known for ratios of scalar quadratic forms [35]. However, the identity in both the numerator and denominator of (40) can be expressed as the limit of a Wishart matrix as in [37]. This gives (40) as the ratio of determinants of matrix quadratic forms which in turn can be decomposed to give a product of scalar quadratic forms as in Appendix B and [38]. Hence, the Laplace approximation for (40) has some motivation in the work of Lieberman [35]. It can also be thought of as a first-order delta expansion [39]. From Appendix C, the expectation in the numerator of (41) is given by

$$E\left\{\left|\sigma^{2}\boldsymbol{I}+\tilde{\boldsymbol{H}}_{k}^{H}\tilde{\boldsymbol{H}}_{k}\right|\right\}=\sum_{i=0}^{k-1}\sum_{\sigma}\operatorname{Perm}\left(\left(\boldsymbol{Q}_{k}\right)^{\sigma_{i,k-1}}\right)\left(\sigma^{2}\right)^{k-i-1},\tag{42}$$

where Q_k is defined in (102). Note that this derivation is not new and is given in [27]. However, it is convenient to include Appendix C so that all required derivations can be found. From Appendix D, the expectation in the denominator of (41) is given by

$$|\mathbf{\Sigma}_k| E\left\{ \left| \sigma^2 \mathbf{I} + \tilde{\mathbf{H}}_k^H \mathbf{\Sigma}_k^{-1} \tilde{\mathbf{H}}_k \right| \right\} = \sum_{l=0}^{n_R} t^l \varphi_{kl}, \quad (43)$$

where φ_{kl} is given in (112). Therefore, $\tilde{I}_k(t)$ becomes

$$\tilde{I}_{k}\left(t\right) \simeq \frac{\Theta\left(\boldsymbol{Q}_{k}\right)}{\sum_{l=0}^{n_{R}} t^{l} \varphi_{kl}} \tag{44}$$

$$= \frac{\Theta\left(\mathbf{Q}_{k}\right)}{\varphi_{kn_{R}} \sum_{l=0}^{n_{R}} \left(\frac{\varphi_{kl}}{\varphi_{kn_{R}}}\right) t^{l}}$$
(45)

$$=\frac{\Theta\left(\boldsymbol{Q}_{k}\right)}{\varphi_{kn,n}\prod_{l=1}^{n_{R}}\left(t+\omega_{kl}\right)},\tag{46}$$

where

$$\Theta\left(\boldsymbol{Q}_{k}\right) = \sum_{i=0}^{k-1} \sum_{\sigma} \operatorname{Perm}\left(\left(\boldsymbol{Q}_{k}\right)^{\sigma_{i,k-1}}\right) \left(\sigma^{2}\right)^{k-i-1}.$$
 (47)

Note that $\omega_{kl} > 0$ for all l, k from Descartes' rule of signs as all the coefficients of the monomial in the denominator of (45) are

positive. Also note that, from (112), we have $\Theta(Q_k) = \varphi_{k0}$. Applying (46) in (39) gives

$$C_k \simeq \int_0^\infty \frac{e^{-t}}{t} - \frac{\varphi_{k0}}{\varphi_{kn_R}} \frac{e^{-t}}{t \prod_{l=1}^{n_R} (t + \omega_{kl})} dt.$$
 (48)

Using a partial fraction expansion for the product in the denominator of the second term of (48) gives

$$\frac{1}{t \prod_{l=1}^{n_R} (t + \omega_{kl})} = \frac{\zeta_{k0}}{t} - \sum_{l=1}^{n_R} \frac{\zeta_{kl}}{t + \omega_{kl}},$$
 (49)

where

$$\zeta_{k0} = \frac{1}{\prod_{u=1}^{n_R} \omega_{ku}} = \frac{\varphi_{kn_R}}{\varphi_{k0}}$$
 (50)

and

$$\zeta_{kl} = \frac{1}{\omega_{kl} \prod_{u \neq l}^{n_R} (\omega_{ku} - \omega_{kl})}.$$
 (51)

Applying (49) in (48) gives

$$C_k \simeq \frac{\varphi_{k0}}{\varphi_{kn_R}} \sum_{l=1}^{n_R} \int_0^\infty \frac{\zeta_{kl}}{t + \omega_{kl}} dt$$
 (52)

$$=\frac{\varphi_{k0}}{\varphi_{kn_R}}\sum_{l=1}^{n_R}\zeta_{kl}e^{\omega_{kl}}E_1\left(\omega_{kl}\right). \tag{53}$$

Then, applying (53) in (36) gives the final approximate ergodic sum rate capacity as

$$E\left\{C\right\} \triangleq \frac{1}{\ln 2} \sum_{k=1}^{N} \left(\frac{\varphi_{k0}}{\varphi_{kn_{R}}} \sum_{l=1}^{n_{R}} \zeta_{kl} e^{\omega_{kl}} E_{1}\left(\omega_{kl}\right)\right). \tag{54}$$

Note the simplicity of the general approximation in (54) in comparison to the two-user exact results in (34).

VI. SIMPLE CAPACITY BOUND

In this section, we consider the simple upper bound given in [27] for the ergodic capacity in (2). This provides a simpler relationship between the average link powers and ergodic sum capacity at the expense of a loss in accuracy.

The result can be given as

$$E\left\{C\right\} \le \log_2\left(\sum_{i=0}^N \sum_{\sigma} \operatorname{Perm}\left(\boldsymbol{P}^{\sigma_{i,N}}\right) \bar{\gamma}^i\right),$$
 (55)

$$= \log_2 \left(\sum_{i=0}^N \vartheta_i \bar{\gamma}^i \right), \tag{56}$$

where ${m P}=(P_{ik})$ and $\bar{\gamma}=\frac{1}{\sigma^2}$. The simplicity of (55) is hidden by the permanent form. For small systems, expanding the permanent reveals the simple relationship between the upper bound and the channel powers. For $n_R=N=2$ and $n_R=N=3$, (56) gives the upper bounds in (57) and (58), shown at the bottom of the page, respectively. These bounds show the simple pattern where cross products of L channel powers scale the $\bar{\gamma}^L$ term. Hence, at low signal-to-noise ratio (SNR) where the $\bar{\gamma}$ term is dominant, $\log_2{(1+P_T\bar{\gamma})}$, where $P_T=\sum_i\sum_k P_{ik}$, is an approximation to (56). Similarly, at high SNR, the $\bar{\gamma}^N$ term is dominant and $\log_2{(1+P\mathrm{erm}\,({\pmb P})\bar{\gamma}^N)}$ is an approximation. These approximations show that capacity is affected by the sum of the channel powers at low SNR, whereas at high SNR, the cross products of N powers become important.

VII. NUMERICAL AND SIMULATION RESULTS

For the numerical results, we consider three distributed BSs with either a single receive antenna or two antennas. For a two-source system, we parameterize the system by three parameters, ρ , ς , and α as in [8] and [9]. The average received SNR is defined by $\rho = P_T/\sigma^2$. In particular for a two-source system, $\rho = (\operatorname{Tr}(\boldsymbol{P}_1) + \operatorname{Tr}(\boldsymbol{P}_2))/\sigma^2$. The total signal-to-interference ratio is defined by $\varsigma = \operatorname{Tr}(\boldsymbol{P}_1)/\operatorname{Tr}(\boldsymbol{P}_2)$. The spread of the signal power across the three BS locations is assumed to follow an exponential profile, as in [37], so that a range of possibilities can be covered with only one parameter. The exponential profile is defined by

$$P_{ik} = K_k(\alpha) \alpha^{i-1}, \tag{59}$$

for receive location $i \in \{1, 2, 3\}$ and source k where

$$K_k(\alpha) = \operatorname{Tr}(\boldsymbol{P}_k) / (1 + \alpha + \alpha^2), \quad k = 1, 2,$$
 (60)

and $\alpha>0$ is the parameter controlling the uniformity of the powers across the antennas. Note that as $\alpha\to 0$, the received power is dominant at the first location, as α becomes large $(\alpha\gg 1)$ the third location is dominant, and as $\alpha\to 1$ there is an even spread, as in the standard microdiversity scenario. Using these parameters, eight scenarios are given in Table I for the case of two single-antenna users. In Fig. 2, we explore the capacity of scenarios S1–S4, where $n_R=3$. The capacity result in (34) agrees with the simulations for all scenarios, thus verifying the exact analysis. Furthermore, the approximation in (54) is shown to be extremely accurate. All capacity results are extremely similar except for S1, where both sources have their dominant path at the first receive antenna. Here, the system

$$E\{C\} \leq \log_{2} \left(1 + \bar{\gamma} \left(P_{11} + P_{12} + P_{21} + P_{22}\right) + \bar{\gamma}^{2} \left(P_{11}P_{22} + P_{12}P_{21}\right)\right)$$

$$E\{C\} \leq \log_{2} \left(1 + \bar{\gamma} \left(P_{11} + P_{12} + P_{13} + P_{21} + P_{22} + P_{23} + P_{31} + P_{32} + P_{33}\right)$$

$$+ \bar{\gamma}^{2} \left(P_{11}P_{22} + P_{11}P_{32} + P_{21}P_{12} + P_{21}P_{32} + P_{31}P_{12} + P_{31}P_{22} + P_{11}P_{23} + P_{11}P_{33} + P_{21}P_{13} \right)$$

$$+ P_{21}P_{33} + P_{31}P_{13} + P_{31}P_{23} + P_{12}P_{23} + P_{12}P_{33} + P_{22}P_{13} + P_{22}P_{33} + P_{32}P_{13} + P_{32}P_{23} \right)$$

$$+ \bar{\gamma}^{3} \left(P_{11}P_{22}P_{33} + P_{11}P_{23}P_{32} + P_{12}P_{21}P_{33} + P_{12}P_{31}P_{23} + P_{13}P_{21}P_{32} + P_{13}P_{22}P_{31}\right)$$

$$(58)$$

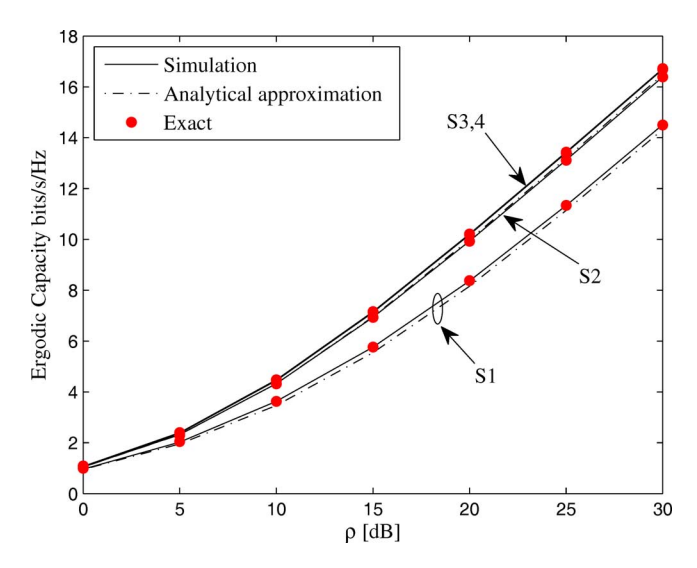


Fig. 2. Exact, approximated, and simulated ergodic sum capacity in flat Rayleigh fading for scenarios S1–S4 with parameters: $n_R=3$, N=W=2, and $\varsigma=1$.

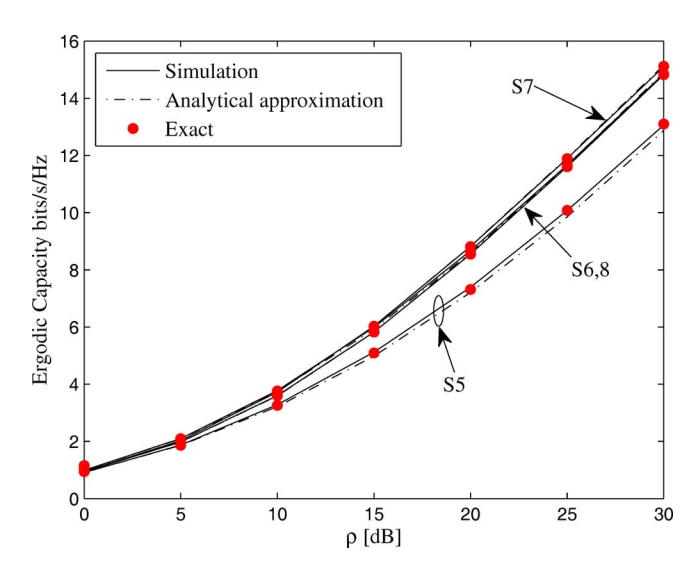


Fig. 3. Exact, approximated, and simulated ergodic sum capacity in flat Rayleigh fading for scenarios S5–S8 with parameters: $n_R=3$, N=W=2, and $\varsigma=10$.

is largely overloaded (two strong signals at a single antenna) and the performance is lower. The similarity of S3 and S4 is interesting as they represent very different systems. In S3, the two users are essentially separated with the dominant channels being at different antennas. In S4, both users have power equally spread over all antennas so the users are sharing all available channels. Fig. 3 follows the same pattern with S6 (the overloaded case) being lower and the other scenarios almost equivalent. In Fig. 3, the overall capacity level is reduced in comparison to Fig. 2 as $\varsigma = 10$ implies a weaker second source.

Figs. 4 and 5 show results for a random drop scenario with $M=n_R=3, W=N=3$, and $n_R=6, M=3, W=N=6$, respectively. In each random drop, uniform random locations are created for the users and lognormal shadow fading and path loss are considered, where $\sigma_{\rm SF}=8$ dB (standard deviation of shadow fading) and $\gamma=3.5$ (path loss exponent). The transmit

TABLE I PARAMETERS FOR FIGS. 2 AND 3

	Decay Parameter		
Sc. No.	User 1	User 2	ς
S1	$\alpha = 0.1$	$\alpha = 0.1$	1
S2	$\alpha = 0.1$	$\alpha = 1$	1
S3	$\alpha = 0.1$	$\alpha = 10$	1
S4	$\alpha = 1$	$\alpha = 1$	1
S5	$\alpha = 0.1$	$\alpha = 0.1$	10
S6	$\alpha = 0.1$	$\alpha = 1$	10
S 7	$\alpha = 0.1$	$\alpha = 10$	10
S 8	$\alpha = 1$	$\alpha = 0.1$	10

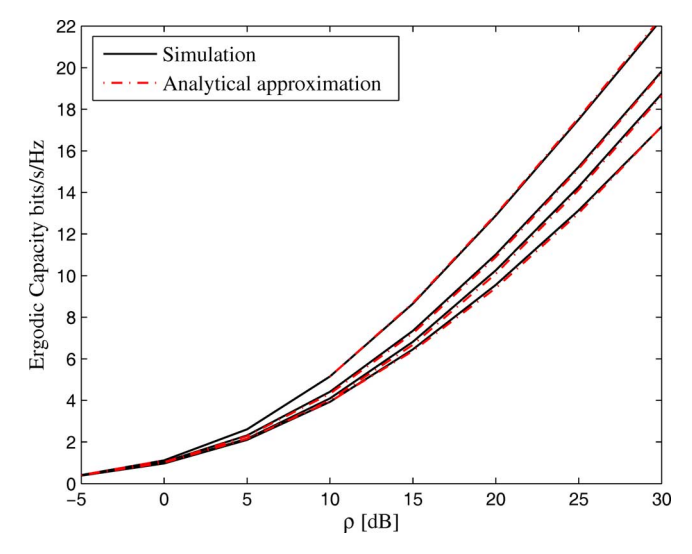


Fig. 4. Approximated and simulated ergodic sum capacity in flat Rayleigh fading for $M=n_R=3,\,W=N=3,$ and four random drops.

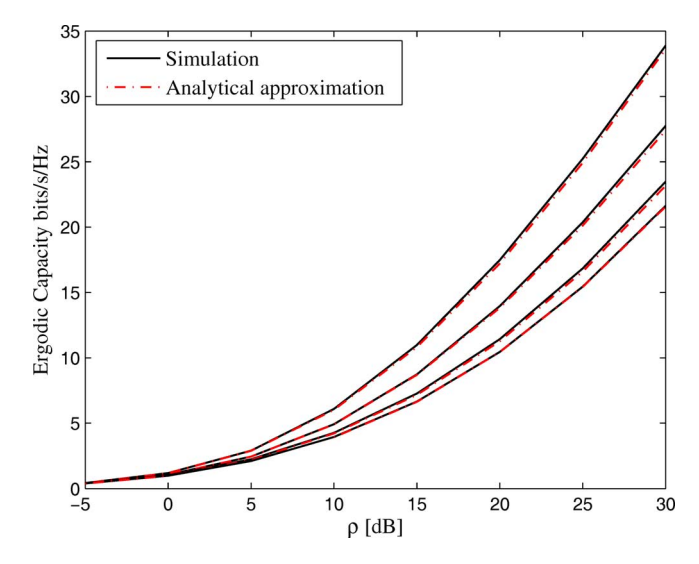


Fig. 5. Approximated and simulated ergodic sum capacity in flat Rayleigh fading for $n_R = 6$, M = 3, W = N = 6, and four random drops.

power of the sources is scaled so that all locations in the coverage area have a maximum received SNR greater than 3 dB, at least 95% of the time. The maximum SNR is taken over the three BSs. Hence, each drop produces a different *P* matrix and independent channels are assumed. The excellent agreement between the approximation in (54) and the simulations in both

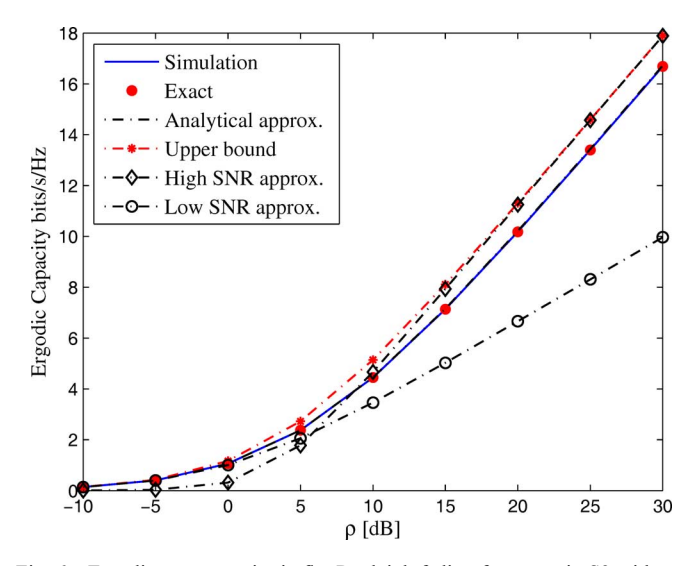


Fig. 6. Ergodic sum capacity in flat Rayleigh fading for scenario S3 with parameters: $M = n_R = 3$, W = N = 2, and $\varsigma = 1$.

Figs. 4 and 5 is encouraging as this demonstrates the accuracy of (54) over different system sizes as well as over completely different sets of channel powers. Note that at high SNR, Fig. 5 gives much higher capacity values than Fig. 4 since there are six receive antenna rather than three. In this high-SNR region, the $\bar{\gamma}^N$ term in (56) dominates and capacity can be approximated by $\log_2 (1 + \text{Perm}(\boldsymbol{P}) \bar{\gamma}^N)$. With $n_R = N = 3$, there are six cross products in Perm (\boldsymbol{P}), whereas with $n_R = N = 6$, there are 720 cross products. Hence, the bound clearly demonstrates the benefits of increased antenna numbers. In practice, there is a tradeoff between the costs of increased collaboration between possibly distant BSs and the resulting increase in system capacity. In Figs. 2-5, at low SNR, the capacity is controlled by P_T . Hence, since $\rho = P_T/\sigma^2$, all four drops have similar performance at low SNR and diverge at higher SNR where the channel profiles affect the results. The upper bound and associated approximations are shown in Figs. 6 and 7 both for a two-user scenario (S3) and a random drop. In Fig. 6, the upper bound is shown for scenario S3 as well as the high- and low-SNR approximations. The results clearly show the loss in accuracy resulting from the use of the simple Jensen bound. However, the bound is quite reasonable over the whole SNR range. The low-SNR approximations are quite reasonable below 0 dB and the high-SNR version is as accurate as the bound above 15 dB. In Fig. 7, similar results are shown for a random drop with $M = n_R = 6, W = N = 6$. Here, similar patterns are observed, but the low- and high-SNR approximations become reasonable at more widely spread SNR values. For example, the low-SNR results are accurate below 0 dB and the high-SNR results are poor until around 30 dB. In contrast, the upper bound is reasonable throughout. Hence, although there is a noticeable capacity error at high SNR, the cross-product coefficients in (57) and (58) are seen to explain the large majority of the ergodic capacity behavior.

In Fig. 8, we compare the accuracy of the proposed approximation in (54) with the approximation based on asymptotic methods found in [21]. In particular, we consider (2,2), (4,4)(6,2), and (5,3) systems with an average channel power of 5 dB

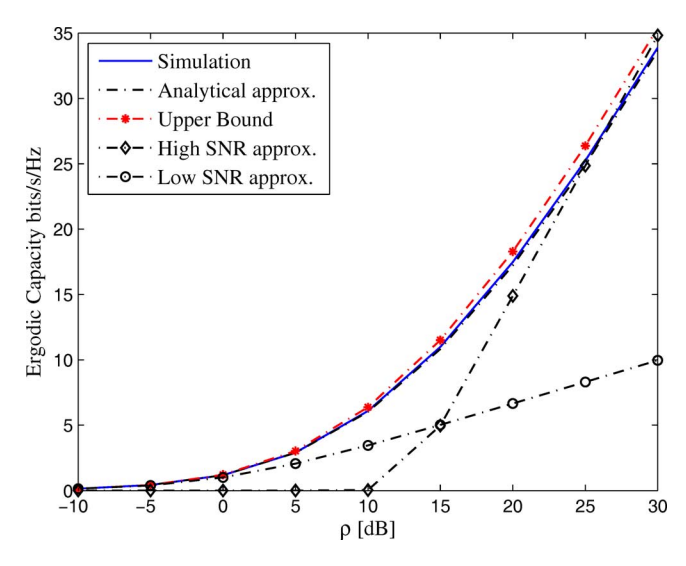


Fig. 7. Ergodic sum capacity in flat Rayleigh fading for a random drop with parameters: $n_R = 6$, M = 3, and W = N = 6.

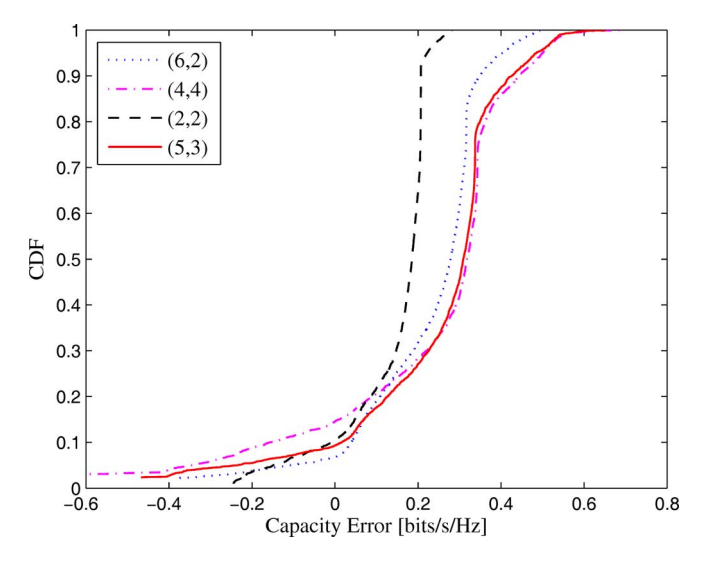


Fig. 8. Simulated capacity error for (2,2), (4,4) (6,2), and (5,3) size systems with an average channel power of 5 dB.

The individual entries of P are generalized as i.i.d. lognormals with a standard deviation of 8 dB. This generates a wide range of P matrices with entries which mimic those encountered in systems experiencing shadow fading. The i.i.d. lognormals are then scaled to give an average link power of 5 dB. The capacity of the MIMO system with a given P matrix is then computed via simulation (using 100 000 trials), using (54) and using (89)–(91) in [21]. This is repeated 10 000 times to give 10 000 errors based on (54), denoted $e_{\rm approx}$, and 10 000 errors based on [21], denoted $e_{\rm asymp}$. The errors are compared via the capacity error defined by $e_{\text{asymp}} - e_{\text{approx}}$. The cumulative distribution function of the capacity error is given in Fig. 8 for four system sizes. We observe that (54) is more accurate than [21] at least 80-90% of the time. Also, increasing asymmetry and reduced system size makes (54) relatively more accurate.

It may be practically important to compare the accuracy of the approximations in terms of the SNR (expressed in dB) required to achieve the same spectral efficiency. Therefore, in Fig. 9, we Authorized licensed use limited to: DUBLIN CITY UNIVERSITY. Downloaded on November 16,2024 at 17:51:24 UTC from IEEE Xplore. Restrictions apply.

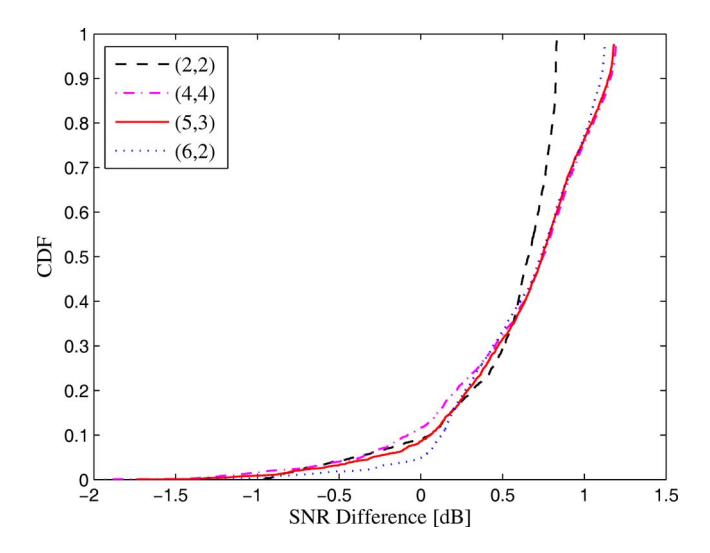


Fig. 9. Simulated SNR difference for (2,2), (4,4), (6,2), and (5,3) size systems with an average channel power of 5 dB.

compare the SNR error of both approximations using 10 000 macrodiversity power profiles (i.e., P matrices). We compute the ergodic capacity of all considered system sizes by simulation at $\bar{\gamma} = 5$ dB. We then reverse calculate the $\bar{\gamma}$ values at which the approximations in [21] and (54) give the above spectral efficiency. This allow us to calculate the SNR error of the approximation proposed in this paper, denoted by $\operatorname{snr}_{\operatorname{approx}}$, and the SNR error of the approximation in [21], denoted by snr_{asymp}. The errors are compared via the SNR difference, defined by $\operatorname{snr}_{\operatorname{asymp}} - \operatorname{snr}_{\operatorname{approx}}$, following the same procedure as in the capacity error analysis in Fig. 8. The cumulative distribution function of the SNR difference is given in Fig. 9 for all system sizes. We observe that the SNR difference also exhibits favorable behavior to the approximation presented in this paper. However, in a vast majority of cases, the difference is less than 1 dB.

VIII. CONCLUSION

In this paper, we have studied the ergodic sum capacity of a Rayleigh fading macrodiversity MIMO-MAC. The results obtained are shown to be valid for both independent channels and correlated channels, which may occur when some of the distributed transmit/receive locations have closely spaced antennas. In particular, we derive exact results for the systems with at most two transmit antennas and approximate results for the general case. The approximations have a simple form and are shown to be very accurate over a wide range of channel powers.

APPENDIX A DERIVATION OF I_b

From (32), I_b can be written as

$$I_b = \frac{\partial \tilde{I}_b}{\partial \theta_1} \bigg|_{\theta_1 = 0},\tag{61}$$

where

$$\tilde{I}_{b} = -\int_{0}^{\infty} \int_{0}^{\infty} \frac{e^{-\sigma^{2}t - \sigma^{2}\theta_{2}}}{\prod_{i=1}^{n_{R}} (1 + tP_{i2} + \theta_{1}P_{i1}P_{i2} + \theta_{2}P_{i1})} d\theta_{2} dt.$$
(62)

From (62), L_b becomes

$$L_{b} = \int_{0}^{\infty} \int_{0}^{\infty} \frac{e^{-\sigma^{2}t - \sigma^{2}\theta_{2}}}{\prod_{i=1}^{n_{R}} \left(\theta_{1} + \frac{\theta_{2}}{P_{i2}} + \frac{t}{P_{i1}} + \frac{1}{P_{i1}P_{i2}}\right)} d\theta_{2} dt.$$
(63)

Defining

$$L_b = -|\boldsymbol{P}_1 \boldsymbol{P}_2| \, \tilde{I}_b, \tag{64}$$

we use a partial fraction expansion in θ_1 to give

$$L_{b} = \sum_{i=1}^{n_{R}} \int_{0}^{\infty} \int_{0}^{\infty} \frac{A_{i}(\theta_{2}, t) e^{-\sigma^{2}t - \sigma^{2}\theta_{2}}}{\left(\theta_{1} + \frac{\theta_{2}}{P_{i2}} + \frac{t}{P_{i1}} + \frac{1}{P_{i1}P_{i2}}\right)} d\theta_{2} dt, \quad (65)$$

where

$$A_i(\theta_2, t) = \frac{1}{\prod_{k \neq i}^{n_R} (\alpha_{ik}\theta_2 + \beta_{ik}t + \gamma_{ik})}$$
(66a)

$$\alpha_{ik} = \frac{1}{P_{k2}} - \frac{1}{P_{i2}}, \quad \beta_{ik} = \frac{1}{P_{k1}} - \frac{1}{P_{i1}} \quad (66b)$$

$$\gamma_{ik} = R_k - R_i, \quad R_i = \frac{1}{P_{i1}P_{i2}}.$$
 (66c)

To compute (65), the following substitutions are employed:

$$u = \sigma^2 t + \sigma^2 \theta_2 \tag{67a}$$

$$v_i = \frac{t}{P_{i1}} + \frac{\theta_2}{P_{i2}}.$$
 (67b)

The Jacobian of the transformation in (67b) can be calculated as

$$J_i = \sigma^2 \left(\frac{1}{P_{i2}} - \frac{1}{P_{i1}} \right). \tag{68}$$

Substituting (67b) and (68) into (65) gives

$$L_{b} = \sum_{i=1}^{n_{R}} \int_{0}^{\infty} \int_{\frac{u}{P_{i1}\sigma^{2}}}^{\frac{u}{P_{i2}\sigma^{2}}} \frac{A_{i}(u, v_{i}) e^{-u}}{J_{i}(v_{i} + \theta_{1} + R_{i})} dv_{i} du,$$
 (69)

where

$$A_{i}(u, v_{i}) = \frac{1}{\prod_{k \neq i}^{n_{R}} (a_{ik}v_{i} + b_{ik}u + \gamma_{ik})}$$
(70a)

$$a_{ik} = \frac{\sigma^2}{J_i} \left(\alpha_{ik} - \beta_{ik} \right) \tag{70b}$$

$$b_{ik} = \frac{1}{J_i} \left(\frac{\beta_{ik}}{P_{i2}} - \frac{\alpha_{ik}}{P_{i1}} \right). \tag{70c}$$

The term $A_i(u, v_i)$ in (70a) can be written as a summation using partial fractions, to give

$$A_{i}(u, v_{i}) = \sum_{k \neq i}^{n_{R}} \frac{B_{ik}(u)}{v_{i} + q_{ik}u + r_{ik}},$$
(71)

where

$$B_{ik}(u) = \frac{(a_{ik})^{n_R - 3}}{\prod_{l \neq i, k}^{n_R} (c_{ikl}u + d_{ikl})}$$
(72a)

$$c_{ikl} = b_{il}a_{ik} - a_{il}b_{ik} (72b)$$

$$d_{ikl} = a_{ik}\gamma_{il} - \gamma_{ik}a_{il} \tag{72c}$$

$$q_{ik} = \frac{b_{ik}}{a_{ik}}, \quad r_{ik} = \frac{\gamma_{ik}}{a_{ik}}.$$
 (72d)

Substituting (71) into (69) and simplifying gives

$$L_{b} = \sum_{i=1}^{n_{R}} \sum_{k \neq i}^{n_{R}} \int_{0}^{\infty} \int_{\frac{u}{P_{i1}\sigma^{2}}}^{\frac{u}{P_{i2}\sigma^{2}}} \frac{B_{ik}(u) e^{-u}}{J_{i}} \times \frac{dv_{i}du}{(v_{i} + \theta_{1} + R_{i})(v_{i} + q_{ik}u + r_{ik})} .$$
(73)

First, we integrate over v_i in (73) to give

$$L_{b} = \sum_{i=1}^{n_{R}} \sum_{k \neq i}^{n_{R}} \int_{0}^{\infty} \frac{C_{ik}(u, \theta_{1}) e^{-u}}{J_{i}} \times \ln \left[\frac{\left(\frac{u}{P_{i2}\sigma^{2}} + \theta_{1} + R_{i}\right)(\lambda_{ik}u + r_{ik})}{\left(\frac{u}{P_{i1}\sigma^{2}} + \theta_{1} + R_{i}\right)(\mu_{ik}u + r_{ik})} \right] du, \quad (74)$$

where

$$C_{ik}\left(u,\theta_{1}\right) = \frac{B_{ik}\left(u\right)}{a_{ik}u + r_{ik} - \theta_{1} - R_{i}} \tag{75a}$$

$$\lambda_{ik} = \frac{1}{P_{i1}\sigma^2} + q_{ik} \tag{75b}$$

$$\mu_{ik} = \frac{1}{P_{i2}\sigma^2} + q_{ik}.\tag{75c}$$

Let

$$D_{ik}(u, \theta_1) = \ln \left[\frac{\left(\frac{u}{P_{i2}\sigma^2} + \theta_1 + R_i\right)(\lambda_{ik}u + r_{ik})}{\left(\frac{u}{P_{i1}\sigma^2} + \theta_1 + R_i\right)(\mu_{ik}u + r_{ik})} \right].$$
(76a)

Then, $B_{ik}(u)$ in (72a) can be rewritten as the summation

$$B_{ik}(u) = \sum_{l \neq i,k}^{n_R} \frac{\xi_{ikl}}{c_{ikl}u + d_{ikl}},$$
(77)

where

$$\xi_{ikl} = \frac{(a_{ik}c_{ikl})^{n_R - 3}}{\prod_{z \neq i, k, l}^{n_R} (d_{ikz}c_{ikl} - c_{ikz}d_{ikl})}.$$
 (78)

Substituting (77) and (75c) into (74) gives

$$L_{b} = \sum_{i=1}^{n_{R}} \sum_{k \neq i}^{n_{R}} \sum_{l \neq i,k}^{n_{R}} \int_{0}^{\infty} D_{ik} (u, \theta_{1}) \frac{\xi_{ikl}}{J_{i}} \times \frac{du}{(c_{ikl}u + d_{ikl}) (q_{ik}u + r_{ik} - \theta_{1} - R_{i})}.$$
(79)

Equation (79) can be further simplified to give

$$L_b = \sum_{i=1}^{n_R} \sum_{k \neq i}^{n_R} \sum_{l \neq i,k}^{n_R} \frac{\xi_{ikl} \left(M_{b_{ikl}} - N_{b_{ikl}} \right)}{J_i}, \tag{80}$$

where

$$M_{b_{ikl}} = \int_0^\infty \frac{D_{ik}(u, \theta_1)}{f_1(\theta_1)} \frac{du}{(u + \varepsilon_{ikl})},\tag{81}$$

$$N_{b_{ikl}} = \int_0^\infty \frac{D_{ik}(u, \theta_1)}{f_1(\theta_1)} \frac{du}{(u + f_2(\theta_1))},$$
 (82)

and $\varepsilon_{ikl} = d_{ikl}/c_{ikl}$. Next, we introduce the following linear functions of θ_1 :

$$f_1(\theta_1) = n_{ikl} - c_{ikl}\theta_1 \tag{83}$$

$$f_2(\theta_1) = m_{ikl} - \frac{\theta_1}{q_{ik}},\tag{84}$$

where

$$n_{ikl} = r_{ik}c_{ikl} - d_{ikl}q_{ik} - \frac{c_{ikl}}{R}.$$
 (85)

$$m_{ikl} = \frac{\gamma_{ik}}{b_{ik}} - \frac{1}{q_{ik}R_i}. (86)$$

Next, we can differentiate $M_{b_{ikl}}$ and $N_{b_{ikl}}$ and integrate over u to give the final result along with (61) and (64). Hence, from (83) and (76a), we get (87). Substituting (87) into (81) and (82), we get (88) and (89). Equations (88) and (89), shown at the bottom of the page, can be solved in closed form to give (90) and (91),

$$\frac{\partial}{\partial \theta_1} \left[\frac{D_{ik} \left(u, \theta_1 \right)}{f_1 \left(\theta_1 \right)} \right]_{\theta_1 = 0} = \frac{c_{ikl}}{n_{ikl}^2} \ln \left[\frac{\left(\frac{u}{P_{i2}\sigma^2} + R_i \right) \left(\lambda_{ik} u + r_{ik} \right)}{\left(\frac{u}{P_{i1}\sigma^2} + R_i \right) \left(\mu_{ik} u + r_{ik} \right)} \right] + \frac{1}{n_{ikl}} \left[\frac{P_{i2}\sigma^2}{\left(u + \frac{\sigma^2}{P_{i1}} \right)} - \frac{P_{i1}\sigma^2}{\left(u + \frac{\sigma^2}{P_{i2}} \right)} \right]$$
(87)

$$\tilde{M}_{b_{ikl}} = \frac{\partial M_{b_{ikl}}}{\partial \theta_1} \bigg|_{\theta_1 = 0} = \int_0^\infty \frac{\partial}{\partial \theta_1} \left[\frac{D_{ik}(u, \theta_1)}{f_1(\theta_1)} \right]_{\theta_1 = 0} \frac{du}{(u + e_{ikl})}$$
(88)

$$\tilde{N}_{b_{ikl}} = \frac{\partial N_{b_{ikl}}}{\partial \theta_1} \bigg|_{\theta_1 = 0} = \int_0^\infty \frac{\partial}{\partial \theta_1} \left[\frac{D_{ik}(u, \theta_1)}{f_1(\theta_1)} \right]_{\theta_1 = 0} \frac{du}{(u + m_{ikl})} + \int_0^\infty \left[\frac{D_{ik}(u, \theta_1)}{f_1(\theta_1)} \right]_{\theta_1 = 0} \frac{1/q_{ik}}{(u + m_{ikl})^2} du \tag{89}$$

shown at the bottom of the page, where we have used the two integrals defined as follows:

$$H_1(a,b,c) = \int_0^\infty \frac{e^{-t} \ln(ct+a)}{t+b} dt$$
$$H_2(a,b,c) = \int_0^\infty \frac{e^{-t} \ln(ct+a)}{(t+b)^2} dt$$

and the constants are given by

$$\varepsilon'_{ikl} = \left(\varepsilon_{ikl} - \frac{\sigma^2}{P_{i1}}\right)^{-1}, \quad \varepsilon''_{ikl} = \left(\varepsilon_{ikl} - \frac{\sigma^2}{P_{i2}}\right)^{-1},$$

$$m'_{ikl} = \left(m_{ikl} - \frac{\sigma^2}{P_{i1}}\right)^{-1}, \quad m''_{ikl} = \left(m_{ikl} - \frac{\sigma^2}{P_{i2}}\right)^{-1}.$$

Both H_1 and H_2 can be solved in closed form as

$$H_1(a,b,c) = e^b \left[E_1(b) \ln c + D_1 \left(\frac{a}{c} - b, b \right) \right],$$

$$H_2(a,b,c) = \ln c \left[\frac{1}{b} - e^b E_1(b) \right] - 2e^b D_1 \left(\frac{a}{c} - b, b \right)$$

$$+ \frac{1}{\left(\frac{a}{c} - b \right)} \left[e^b E_1(b) - e^{\frac{a}{c}} E_1 \left(\frac{a}{c} \right) \right],$$

where $D_1(a, b)$ is defined by

$$D_1(a,b) = \int_b^\infty \frac{e^{-t} \ln(t+a)}{t} dt, \quad \text{for} \quad b \neq 0.$$

APPENDIX B

EXTENDED LAPLACE-TYPE APPROXIMATION

Note the well-known fact that, $\sigma^2 \boldsymbol{I} = E\left\{\boldsymbol{A}^H\boldsymbol{A}\right\}$, for an i.i.d. complex Gaussian matrix ensemble, \boldsymbol{A} , of $\mathcal{CN}\left(0,\frac{\sigma^2}{\kappa}\right)$ random

variables, where \boldsymbol{A} is a $\kappa \times k-1$ matrix as in [37]. This result can be rewritten in the limit to give $\sigma^2 \boldsymbol{I} = \lim_{\kappa \to \infty} \left\{ \boldsymbol{A}^H \boldsymbol{A} \right\}$. Using this in (40) gives

$$\tilde{I}_{k}(t) = \frac{1}{|\mathbf{\Sigma}_{k}|} \lim_{\kappa \to \infty} E \left\{ \frac{\left| \mathbf{A}^{H} \mathbf{A} + \tilde{\mathbf{H}}_{k}^{H} \tilde{\mathbf{H}}_{k} \right|}{\left| \mathbf{A}^{H} \mathbf{A} + \tilde{\mathbf{H}}_{k}^{H} \mathbf{\Sigma}_{k}^{-1} \tilde{\mathbf{H}}_{k} \right|} \right\}, \tag{92}$$

$$= \frac{1}{|\mathbf{\Sigma}_{k}|} \lim_{\kappa \to \infty} E \left\{ \frac{\left| \left(\mathbf{A}^{H}, \tilde{\mathbf{H}}_{k}^{H} \mathbf{\Sigma}_{k}^{-1} \tilde{\mathbf{H}}_{k} \right) \right|}{\left| \left(\mathbf{A}^{H}, \tilde{\mathbf{H}}_{k}^{H} \mathbf{\Sigma}_{k}^{-\frac{1}{2}} \right) \left(\frac{\mathbf{A}}{\mathbf{\Sigma}_{k}^{-\frac{1}{2}} \tilde{\mathbf{H}}_{k}} \right) \right|} \right\}, \tag{93}$$

$$= \frac{1}{|\mathbf{\Sigma}_{k}|} \lim_{\kappa \to \infty} E \left\{ \frac{\left| \mathbf{B}_{k}^{H} \mathbf{B}_{k} \right|}{\left| \mathbf{B}_{k}^{H} \tilde{\mathbf{\Sigma}}_{k} \mathbf{B}_{k} \right|} \right\}, \tag{94}$$

where $\bar{\Sigma}_k = \mathrm{diag}\left(I, \Sigma_{\pmb{k}}^{-\frac{1}{2}}\right)$ and $B_k = \begin{pmatrix} \pmb{A} \\ \hat{\pmb{H}}_k \end{pmatrix}$. Using the well-known fact

$$\left| \boldsymbol{B}_{k}^{H} \boldsymbol{B}_{k} \right| = \prod_{i=1}^{k-1} \boldsymbol{b}_{ki}^{H} \left(\boldsymbol{I} - \tilde{\boldsymbol{B}}_{ki} \left(\tilde{\boldsymbol{B}}_{ki}^{H} \tilde{\boldsymbol{B}}_{ki} \right)^{-1} \tilde{\boldsymbol{B}}_{ki}^{H} \right) \boldsymbol{b}_{ki}, \quad (95)$$

from standard linear algebra, where \boldsymbol{b}_{ki} is the ith column of \boldsymbol{B}_k , $\tilde{\boldsymbol{B}}_{ki}$ is \boldsymbol{B}_k with columns $1,2\ldots i-1$, $\left|\tilde{\boldsymbol{B}}_{k1}^H\tilde{\boldsymbol{B}}_{k1}\right|=1$ and $\tilde{\boldsymbol{B}}_{k1}\left(\tilde{\boldsymbol{B}}_{k1}^H\tilde{\boldsymbol{B}}_{k1}\right)^{-1}\tilde{\boldsymbol{B}}_{k1}^H=0$, we can approximate (94) by the expression in (96), shown at the bottom of the page, where \boldsymbol{b}_{ki} and \boldsymbol{B}_k correspond to a large but finite value of κ . Approximation (96) assumes that the terms in the product in (95) are independent. This is only true when \boldsymbol{b}_{ki} contains i.i.d. elements. However, in the macrodiversity case, all the elements of \boldsymbol{b}_{ki} are not i.i.d. Nevertheless, part of \boldsymbol{b}_{ki} (the contribution from \boldsymbol{A}) is i.i.d. This motivates the approximation in (96). Next, we apply the standard Laplace type approximation [35] in (96) to give (97)–(99). Hence, a combination of approximate independence, the Laplace approximation for quadratic forms and the limiting version in (92) gives rise to the approximation used in Section V.

$$\tilde{M}_{b_{ikl}} = \frac{c_{ikl}}{n_{ikl}^2} \left[H_1 \left(R_i, \varepsilon_{ikl}, \frac{1}{P_{i2}\sigma^2} \right) + H_1 \left(r_{ik}, \varepsilon_{ikl}, \lambda_{ik} \right) - H_1 \left(R_i, \varepsilon_{ikl}, \frac{1}{P_{i1}\sigma^2} \right) - H_1 \left(r_{ik}, \varepsilon_{ikl}, \mu_{ik} \right) \right]
+ \frac{\varepsilon'_{ikl}}{n_{ikl}} \left[e^{\frac{\sigma^2}{P_{i1}}} E_1 \left(\frac{\sigma^2}{P_{i1}} \right) - e^{\varepsilon_{ikl}} E_1 \left(\varepsilon_{ikl} \right) \right] - \frac{\varepsilon''_{ikl}}{n_{ikl}} \left[e^{\frac{\sigma^2}{P_{i2}}} E_1 \left(\frac{\sigma^2}{P_{i2}} \right) - e^{\varepsilon_{ikl}} E_1 \left(\varepsilon_{ikl} \right) \right]$$
(90)

$$\tilde{N}_{b_{ikl}} = \frac{c_{ikl}}{n_{ikl}^2 q_{ik}} \left[H_2 \left(R_i, m_{ikl}, \frac{1}{P_{i2}\sigma^2} \right) + H_2 \left(r_{ik}, m_{ikl}, \lambda_{ik} \right) - H_2 \left(R_i, m_{ikl}, \frac{1}{P_{i1}\sigma^2} \right) - H_2 \left(r_{ik}, m_{ikl}, \mu_{ik} \right) \right]
+ \frac{c_{ikl}}{n_{ikl}^2} \left[H_1 \left(R_i, m_{ikl}, \frac{1}{P_{i2}\sigma^2} \right) + H_1 \left(r_{ik}, m_{ikl}, \lambda_{ik} \right) - H_1 \left(R_i, m_{ikl}, \frac{1}{P_{i1}\sigma^2} \right) - H_1 \left(r_{ik}, m_{ikl}, \mu_{ik} \right) \right]
+ \frac{m'_{ikl}}{n_{ikl}} \left[e^{\frac{\sigma^2}{P_{i1}}} E_1 \left(\frac{\sigma^2}{P_{i1}} \right) - e^{m_{ikl}} E_1 \left(m_{ikl} \right) \right] - \frac{m''_{ikl}}{n_{ikl}} \left[e^{\frac{\sigma^2}{P_{i2}}} E_1 \left(\frac{\sigma^2}{P_{i2}} \right) - e^{m_{ikl}} E_1 \left(m_{ikl} \right) \right]$$
(91)

$$\tilde{I}_{k}(t) \simeq \frac{1}{|\Sigma_{k}|} \prod_{i=1}^{k-1} E \left\{ \frac{\boldsymbol{b}_{ki}^{H} \left(\boldsymbol{I} - \tilde{\boldsymbol{B}}_{ki} \left(\tilde{\boldsymbol{B}}_{ki}^{H} \tilde{\boldsymbol{B}}_{ki} \right)^{-1} \tilde{\boldsymbol{B}}_{ki}^{H} \right) \boldsymbol{b}_{ki}}{\boldsymbol{b}_{ki}^{H} \left(\tilde{\Sigma}_{k} - \tilde{\Sigma}_{k} \tilde{\boldsymbol{B}}_{ki} \left(\tilde{\boldsymbol{B}}_{ki}^{H} \tilde{\Sigma}_{k} \tilde{\boldsymbol{B}}_{ki} \right)^{-1} \tilde{\boldsymbol{B}}_{ki}^{H} \tilde{\Sigma}_{k} \right) \boldsymbol{b}_{ki}} \right\}$$
(96)

The accuracy of this approach is numerically established in the simulation results in Section VII.

APPENDIX C

Calculation of
$$E\left\{ \left| \sigma^2 \pmb{I} + \tilde{\pmb{H}}_k^H \tilde{\pmb{H}}_k \right| \right\}$$

This appendix is included for completeness. Original derivation can be found in [27]. Let $\lambda_1, \lambda_2, \dots, \lambda_{k-1}$ be the ordered eigenvalues of $\tilde{\boldsymbol{H}}_{k}^{H}\tilde{\boldsymbol{H}}_{k}$. Since $n_{R} \geq (k-1)$, all eigenvalues

$$E\left\{\left|\sigma^{2}\boldsymbol{I}+\tilde{\boldsymbol{H}}_{k}^{H}\tilde{\boldsymbol{H}}_{k}\right|\right\} = E\left\{\prod_{i=1}^{k-1}\left(\sigma^{2}+\lambda_{i}\right)\right\}$$

$$=E\left\{\sum_{i=0}^{k-1}\operatorname{Tr}_{i}\left(\tilde{\boldsymbol{H}}_{k}^{H}\tilde{\boldsymbol{H}}_{k}\right)\left(\sigma^{2}\right)^{k-i-1}\right\},$$
(100)

where (100) is from (8) and Lemma 2. Therefore, the building block of this expectation is $E\left\{\operatorname{Tr}_i\left(\tilde{\boldsymbol{H}}_k^H\tilde{\boldsymbol{H}}_k\right)\right\}$. From Lemma

$$\operatorname{Tr}_{i}\left(\tilde{\boldsymbol{H}}_{k}^{H}\tilde{\boldsymbol{H}}_{k}\right) = \sum_{\sigma} \left| \left(\tilde{\boldsymbol{H}}_{k}^{H}\tilde{\boldsymbol{H}}_{k}\right)_{\sigma_{i,k-1}} \right|. \tag{101}$$

Therefore, from Lemma 1

$$E\left\{\operatorname{Tr}_{i}\left(\tilde{\boldsymbol{H}}_{k}^{H}\tilde{\boldsymbol{H}}_{k}\right)\right\} = \sum_{\sigma}\operatorname{Perm}\left(\left(\boldsymbol{Q}_{k}\right)^{\sigma_{i,k-1}}\right),$$

where the $n_R \times (k-1)$ matrix, Q_k , is given by

$$E\left\{\tilde{\boldsymbol{H}}_{k}\circ\bar{\tilde{\boldsymbol{H}}}_{k}\right\} = \boldsymbol{Q}_{k}.\tag{102}$$

Note that summation in (102) has $\binom{k-1}{i}$ terms. Then, the final expression becomes

$$E\left\{\left|\sigma^{2}\boldsymbol{I}+\tilde{\boldsymbol{H}}_{k}^{H}\tilde{\boldsymbol{H}}_{k}\right|\right\} = \sum_{i=0}^{k-1} \sum_{\sigma} \operatorname{Perm}\left(\left(\boldsymbol{Q}_{k}\right)^{\sigma_{i,k-1}}\right) \left(\sigma^{2}\right)^{k-i-1}.$$

$$\left|\left(\boldsymbol{\Sigma}_{k}\right)_{\bar{\sigma}_{n_{R}-i,n_{R}}}\right| = \sum_{l=0}^{n_{R}-i} \left(\frac{t}{\sigma^{2}}\right)^{l} \operatorname{Tr}_{l}\left(\left(\boldsymbol{P}_{k}\right)_{\bar{\sigma}_{n_{R}-i,n_{R}}}\right). \quad (109)$$

APPENDIX D

CALCULATION OF
$$\left| \mathbf{\Sigma}_k \right| E \left\{ \left| \sigma^2 \mathbf{I} + \tilde{\mathbf{H}}_k^H \mathbf{\Sigma}_k^{-1} \tilde{\mathbf{H}}_k \right| \right\}$$

A simple extension of (42) allows the expectation in the denominator of (41) to be calculated as

$$E\left\{\left|\sigma^{2}\boldsymbol{I}+\tilde{\boldsymbol{H}}_{k}^{H}\boldsymbol{\Sigma}_{k}^{-1}\tilde{\boldsymbol{H}}_{k}\right|\right\}=\sum_{i=0}^{k-1}\psi_{ki}\left(t\right)\left(\sigma^{2}\right)^{k-i-1},\quad(104)$$

where

$$\psi_{ki}(t) = \sum_{\sigma} \operatorname{Perm}\left(\left(\boldsymbol{\Sigma}_{k}^{-1} \boldsymbol{Q}_{k}\right)^{\sigma_{i,k-1}}\right), \quad (105)$$

and from (12)

$$\psi_{k0}\left(t\right) = 1.$$

The term in (105) can be simplified using (13) to obtain

$$\psi_{ki}(t) = \sum_{\sigma} \frac{\operatorname{Perm}\left((\boldsymbol{Q}_{k})_{\sigma_{i,n_{R}}}^{\{k-1\}}\right)}{\left|(\boldsymbol{\Sigma}_{k})_{\sigma_{i,n_{R}}}\right|}.$$
 (106)

Then,

$$\left| \mathbf{\Sigma}_{k} \right| E \left\{ \left| \sigma^{2} \mathbf{I} + \tilde{\mathbf{H}}_{k}^{H} \mathbf{\Sigma}_{k}^{-1} \tilde{\mathbf{H}}_{k} \right| \right\} = \sum_{i=0}^{k-1} \xi_{ki} \left(t \right) \left(\sigma^{2} \right)^{k-i-1},$$

$$(107)$$

where $\xi_{ki}(t) = |\mathbf{\Sigma}_k| \psi_{ki}(t)$. From (106), we obtain

$$\xi_{ki}(t) = \sum_{\sigma} \left| (\boldsymbol{\Sigma}_k)_{\bar{\sigma}_{n_R-i,n_R}} \right| \operatorname{Perm}\left((\boldsymbol{Q}_k)_{\sigma_{i,n_R}}^{\{k-1\}} \right), \quad (108)$$

where $\bar{\sigma}_{n_R-i,n_R}$ is the compliment of σ_{i,n_R} . Therefore, it is apparent that $\xi_{ki}(t)$ is a polynomial of degree $n_R - i$. Clearly $|\mathbf{\Sigma}_k| E\left\{\left|\sigma^2 \mathbf{I} + \tilde{\mathbf{H}}_k^H \mathbf{\Sigma}_k^{-1} \tilde{\mathbf{H}}_k\right|\right\}$ is a polynomial of degree n_R , since $\xi_{k0}(t) = |\mathbf{\Sigma}_k|$ is the highest degree polynomial term in tin (107). Then,

$$\left| (\boldsymbol{\Sigma}_k)_{\bar{\sigma}_{n_R-i,n_R}} \right| = \sum_{l=0}^{n_R-i} \left(\frac{t}{\sigma^2} \right)^l \operatorname{Tr}_l \left((\boldsymbol{P}_k)_{\bar{\sigma}_{n_R-i,n_R}} \right). \tag{109}$$

$$\tilde{I}_{k}(t) \simeq \frac{1}{|\Sigma_{k}|} \prod_{i=1}^{k-1} \frac{E\left\{\boldsymbol{b}_{ki}^{H}\left(\boldsymbol{I} - \tilde{\boldsymbol{B}}_{ki}\left(\tilde{\boldsymbol{B}}_{ki}^{H}\tilde{\boldsymbol{B}}_{ki}\right)^{-1}\tilde{\boldsymbol{B}}_{ki}^{H}\right)\boldsymbol{b}_{ki}\right\}}{E\left\{\boldsymbol{b}_{ki}^{H}\left(\bar{\boldsymbol{\Sigma}}_{k} - \bar{\boldsymbol{\Sigma}}_{k}\tilde{\boldsymbol{B}}_{ki}\left(\tilde{\boldsymbol{B}}_{ki}^{H}\bar{\boldsymbol{\Sigma}}_{k}\tilde{\boldsymbol{B}}_{ki}\right)^{-1}\tilde{\boldsymbol{B}}_{ki}^{H}\bar{\boldsymbol{\Sigma}}_{k}\right)\boldsymbol{b}_{ki}\right\}},$$
(97)

$$\simeq \frac{1}{|\mathbf{\Sigma}_{k}|} \frac{E\left\{\prod_{i=1}^{k-1} \boldsymbol{b}_{ki}^{H} \left(\boldsymbol{I} - \tilde{\boldsymbol{B}}_{ki} \left(\tilde{\boldsymbol{B}}_{ki}^{H} \tilde{\boldsymbol{B}}_{ki}\right)^{-1} \tilde{\boldsymbol{B}}_{ki}^{H}\right) \boldsymbol{b}_{ki}\right\}}{E\left\{\prod_{i=1}^{k-1} \boldsymbol{b}_{ki}^{H} \left(\bar{\boldsymbol{\Sigma}}_{k} - \bar{\boldsymbol{\Sigma}}_{k} \tilde{\boldsymbol{B}}_{ki} \left(\tilde{\boldsymbol{B}}_{ki}^{H} \bar{\boldsymbol{\Sigma}}_{k} \tilde{\boldsymbol{B}}_{ki}\right)^{-1} \tilde{\boldsymbol{B}}_{ki}^{H} \bar{\boldsymbol{\Sigma}}_{k}\right) \boldsymbol{b}_{ki}\right\}},$$
(98)

$$= \frac{1}{|\mathbf{\Sigma}_k|} \frac{E\{|\mathbf{B}_k^H \mathbf{B}_k|\}}{E\{|\mathbf{B}_k^H \bar{\mathbf{\Sigma}}_k \mathbf{B}_k|\}}.$$
(99)

Hence, applying (109) in (108),

 $\xi_{ki}(t)$

$$= \sum_{\sigma} \sum_{l=0}^{n_R-i} \left(\frac{t}{\sigma^2}\right)^l \operatorname{Tr}_l\left((\boldsymbol{P}_k)_{\bar{\sigma}_{n_R-i,n_R}}\right) \operatorname{Perm}\left((\boldsymbol{Q}_k)_{\sigma_{i,n_R}}^{\{k-1\}}\right),$$

and $\xi_{ki}(t)$ becomes

$$\xi_{ki}(t) = \sum_{l=0}^{n_R - i} \left(\frac{t}{\sigma^2}\right)^l \hat{\varphi}_{kli}$$
 (110)

$$=\sum_{l=0}^{n_R} \left(\frac{t}{\sigma^2}\right)^l \hat{\varphi}_{kli},\tag{111}$$

where

$$\hat{\varphi}_{kli} = \sum_{\boldsymbol{\sigma}} \operatorname{Tr}_{l} \left((\boldsymbol{P}_{k})_{\bar{\sigma}_{n_{R}-i,n_{R}}} \right) \operatorname{Perm} \left((\boldsymbol{Q}_{k})_{\sigma_{i,n_{R}}}^{\{k-1\}} \right),$$

and from (12), $\hat{\varphi}_{kl0}$ simplifies to give

$$\hat{\varphi}_{kl0} = \operatorname{Tr}_{l}\left(\boldsymbol{P}_{k}\right).$$

Equation (111) follows from (110) due to the fact that

$$\operatorname{Tr}_l\left((\boldsymbol{P}_k)_{\bar{\sigma}_{n_R-i,n_R}}\right) = 0 \quad \text{for} \quad l > n_R - i.$$

Therefore, (104) can be written as

$$\left| \boldsymbol{\Sigma}_{k} \right| E \left\{ \left| \sigma^{2} \boldsymbol{I} + \tilde{\boldsymbol{H}}_{k}^{H} \boldsymbol{\Sigma}_{k}^{-1} \tilde{\boldsymbol{H}}_{k} \right| \right\} = \sum_{i=0}^{k-1} \sum_{l=0}^{n_{R}} t^{l} \, \hat{\varphi}_{kli} \left(\sigma^{2} \right)^{k-l-i-1},$$

which, in turn, can be given as

$$\left| \boldsymbol{\Sigma}_{k} \right| E \left\{ \left| \sigma^{2} \boldsymbol{I} + \tilde{\boldsymbol{H}}_{k}^{H} \boldsymbol{\Sigma}_{k}^{-1} \tilde{\boldsymbol{H}}_{k} \right| \right\} = \sum_{l=0}^{n_{R}} t^{l} \varphi_{kl},$$

where

$$\varphi_{kl} = \sum_{i=0}^{k-1} \hat{\varphi}_{kli} \left(\sigma^2\right)^{k-l-i-1}.$$
 (112)

ACKNOWLEDGMENT

The authors would like to thank Associate Editor, Prof. A. Lozano, for his constructive criticisms during the entire course of review of this paper.

REFERENCES

- S. Venkatesan, A. Lozano, and R. Valenzuela, "Network MIMO: Overcoming intercell interference in indoor wireless systems," in *Proc. IEEE Asilomar Conf. Signals, Syst., Comput.*, Pacific Grove, CA, USA, Jul. 2007, pp. 83–87.
- [2] M. K. Karakayali, G. J. Foschini, and R. A. Valenzuela, "Network coordination for spectrally efficient communications in cellular systems," *IEEE Trans. Wireless Commun.*, vol. 13, no. 4, pp. 56–61, Aug. 2006.

- [3] E. Biglieri, R. Calderbank, A. Constantinides, A. Goldsmith, A. Paulraj, and H. V. Poor, MIMO Wireless Communication, 1st ed. Cambridge, U.K.: Cambridge Univ. Press, 2007.
- [4] A. Papadogiannis, D. Gesbert, and E. Hardouin, "A dynamic clustering approach in wireless networks with multi-cell cooperative processing," in *Proc. IEEE Int. Conf. Commun.*, Beijing, China, 2008, pp. 4033–4037
- [5] E. Aktas, J. Evans, and S. Hanly, "Distributed decoding in a cellular multiple-access channel," in *Proc. IEEE Int. Symp. Inf. Theory*, Chicago, IL, USA, Jun. 2004, pp. 484–488.
- [6] M. N. Bacha, J. S. Evans, and S. V. Hanly, "On the capacity of cellular networks with MIMO links," in *Proc. IEEE Int. Conf. Commun.*, Istanbul, Turkey, Jun. 2004, pp. 1337–1342.
- [7] O. Somekh, B. M. Zaidel, and S. Shamai (Shitz), "Spectral efficiency of joint multiple cellsite processors for randomly spread DS-CDMA systems," *IEEE Trans. Inf. Theory*, vol. 53, no. 7, pp. 2625–2637, Jul. 2007
- [8] D. A. Basnayaka, P. J. Smith, and P. A. Martin, "Symbol error rate performance for macrodiversity maximal ratio combining in flat Rayleigh fading," in *Proc. IEEE Australian Commun. Theory Workshop*, Wellington, New Zealand, 2012, pp. 25–30.
- [9] D. A. Basnayaka, P. J. Smith, and P. A. Martin, "Exact dual-user macrodiversity performance with linear receivers in flat Rayleigh fading," in *Proc. IEEE Int. Conf. Commun.*, Ottawa, ON, Canada, Jun. 2012, pp. 5626–5631.
- [10] M. Kiessling and J. Speidel, "Mutual information of MIMO channels in correlated Rayleigh fading environments—A general solution," in *Proc. IEEE Int. Conf. Commun.*, Paris, France, 2004, vol. 2, pp. 814–818.
- [11] W. Choi and J. G. Andrews, "Downlink performance and capacity of distributed antenna systems in a multicell environment," *IEEE Trans. Wireless Commun.*, vol. 6, no. 1, pp. 69–73, Jan. 2007.
- [12] X. Yu, X. Liu, Y. Xin, M. Chen, and Y. Rui, "Capacity analysis of distributed antenna systems with multiple receive antennas over MIMO fading channel," *Int. J. Antenn. Propag.*, vol. 2012, pp. 409254-1–409254-7, 2012.
- [13] S. Firouzabadi and A. Goldsmith, "Downlink performance and capacity of distributed antenna systems," 2011 [Online]. Available: http://arxiv.org/pdf/1109.2957v1.pdf
- [14] S. V. Hanly, "Capacity and power control in spread spectrum macrodiversity radio networks," *IEEE Trans. Commun.*, vol. 44, no. 2, pp. 247–256, Feb. 1996.
- [15] W. Hachem, P. Loubaton, and J. Najim, "Deterministic equivalents for certain functionals of large random matrices," *Ann. Appl. Probab.*, vol. 17, no. 3, pp. 875–930, 2007.
- [16] W. Hachem, O. Khorunzhiy, P. Loubaton, J. Najim, and L. Pastur, "A new approach for capacity analysis for large dimensional multi-antenna channels," *IEEE Trans. Inf. Theory*, vol. 54, no. 9, pp. 3987–4004, Sep. 2008
- [17] S. Chatzinotas, M. Imran, and R. Hoshyar, "On the multicell processing capacity of the cellular MIMO uplink channel in correlated Rayleigh fading environment," *IEEE Trans. Wireless Commun.*, vol. 8, no. 7, pp. 3704–3715, Jul. 2009.
- [18] C. K. Wen, K. K. Wong, and J. C. Chen, "Spatially correlated MIMO multiple-access systems with macrodiversity: Asymptotic analysis via statistical physics," *IEEE Trans. Commun.*, vol. 55, no. 3, pp. 477–488, Mar. 2007.
- [19] L. Dai, "A comparative study on uplink sum capacity with co-located and distributed antennas," *IEEE J. Sel. Areas Commun.*, vol. 29, no. 6, pp. 1200–1213, Jun. 2011.
- [20] L. Dai, "Distributed antenna system: Performance analysis in multiuser scenario," in *Proc. IEEE Conf. Inf. Sci. Syst.*, Princeton, NJ, USA, Mar. 2008, pp. 85–89.
- [21] A. M. Tulino, A. Lozano, and S. Verdu, "Impact of antenna correlation on the capacity of multiantenna channels," *IEEE Trans. Inf. Theory*, vol. 51, no. 7, pp. 2491–2509, Jul. 2005.
- [22] W. Weichselberger, M. Herdin, H. Ozcelik, and E. Bonek, "A sto-chastic MIMO channel model with joint correlation of both link ends," *IEEE Trans. Wireless Commun.*, vol. 5, no. 1, pp. 90–100, Jan. 2006.
- [23] E. Telatar, "Capacity of multi-antenna Gaussian channels," Eur. Trans. Telecommun., vol. 10, no. 6, pp. 585–595, 1999.

- [24] H. Shin, M. Z. Win, J. H. Lee, and M. Chiani, "On the capacity of doubly correlated MIMO channels," *IEEE Trans. Wireless Commun.*, vol. 5, no. 8, pp. 2253–2265, Aug. 2006.
- [25] D. A. Basnayaka, P. J. Smith, and P. A. Martin, "Ergodic sum capacity of macrodiversity MIMO systems in flat Rayleigh fading," in *Proc. IEEE Int. Symp. Inf. Theory*, Cambridge, MA, USA, Jul. 2012, pp. 2181–2185.
- [26] D. Shiu, G. Foschini, M. Gans, and J. Kahn, "Fading correlation and its effect on the capacity of multielement antenna systems," *IEEE Trans. Commun.*, vol. 48, no. 3, pp. 502–513, Mar. 2000.
- [27] X. Q. Gao, B. Jiang, X. Li, A. B. Gershman, and M. R. McKay, "Statistical eigenmode transmission over jointly correlated MIMO channels," *IEEE Trans. Inf. Theory*, vol. 55, no. 8, pp. 3735–3750, Aug. 2009.
- [28] H. Minc, *Permanants*, 1st ed. Reading, MA, USA: Addison-Wesley, 1978
- [29] R. J. Muirhead, Aspects of Multivariate Statistical Theory, 1st ed. New York, NY, USA: Wiley, 1982.
- [30] A. Paulraj, R. Nabar, and D. Gore, Introduction to Space-Time Wireless Communication, 1st ed. Cambridge, U.K.: Cambridge Univ. Press, 2007.
- [31] H. Lütkepohl, Handbook of Matrices, 1st ed. New York, NY, USA: Wiley, 1996.
- [32] D. Hammarwall, M. Bengtsson, and B. Ottersten, "Acquiring partial CSI for spatially selective transmission by instantaneous channel norm feedback," *IEEE Trans. Signal Process.*, vol. 56, no. 3, pp. 1188–1204, Mar. 2008.
- [33] V. Raghavan, S. V. Hanly, and V. V. Veeravalli, "Statistical beamforming on the Grassmann manifold for the two-user broadcast channel," 2011 [Online]. Available: http://arxiv.org/abs/1104.2116
- [34] I. S. Gradshteyn and I. M. Ryzhik, *Table of Integrals, Series, and Products*, 6rd ed. Boston, MA, USA: Academic, 2000.
- [35] O. Lieberman, "A Laplace approximation to the moments of a ratio of quadratic forms," *Biometrika*, vol. 81, no. 4, pp. 681–690, Dec. 1994.
- [36] T. M. Cover and J. A. Thomas, Elements of Information Theory, 3rd ed. New York, NY, USA: Wiley, 1991.
- [37] H. Gao, P. J. Smith, and M. V. Clark, "Theoretical reliability of MMSE linear diversity combining in Rayleigh-fading additive interference channels," *IEEE Trans. Commun.*, vol. 46, no. 5, pp. 666–672, May 1998.
- [38] D. A. Basnayaka, "Macrodiversity MIMO transceivers," Ph.D. dissertation, Dept. Electr. Comput. Eng., Univ. Canterbury, Christchurch, New Zealand, Jun. 2012.
- [39] A. Stuart and J. K. Ord, Kendall's Advanced Theory of Statistics: Volume 1 Distribution Theory, 6th ed. London, U.K.: Edward Arnold, 1994.

Dushyantha A. Basnayaka (S'11–M'12) received the B.Sc.Eng degree with 1st class honors from the University of Peradeniya, Sri Lanka, in 2006. He received the Ph.D. degree in electrical and computer engineering from the University of Canterbury, Christchurch, New Zealand, in 2012.

He was a system engineer at MillenniumIT (a member company of London Stock Exchange group) from 2006 to 2009. He was with the communication research group at the University of Canterbury, New Zealand from 2009 until 2012. He is now with Institute for Digital Communication at the University of Edinburgh, United Kingdom.

Dr. Basnayaka was a recipient of University of Canterbury International Doctoral Scholarship for his doctoral studies at UC. His current research interest includes massive MIMO, spatial modulation, visible light communication (VLC) and, macrodiversity MU-MIMO systems.

Peter J. Smith (M'93–SM'01) received the B.Sc degree in Mathematics and the Ph.D. degree in Statistics from the University of London, London, U.K., in 1983 and 1988, respectively. From 1983 to 1986 he was with the Telecommunications Laboratories at GEC Hirst Research Centre. From 1988 to 2001 he was a lecturer in statistics at Victoria University, Wellington, New Zealand. Since 2001 he has been a Senior Lecturer and Associate Professor in Electrical and Computer Engineering at the University of Canterbury in New Zealand. Currently, he is a full Professor at the same department.

His research interests include the statistical aspects of design, modeling and analysis for communication systems, especially antenna arrays, MIMO, cognitive radio and relays.

Philippa A. Martin (S'95–M'01–SM'06) received the B.E. (Hons. 1) and Ph.D. degrees in electrical and electronic engineering from the University of Canterbury, Christchurch, New Zealand, in 1997 and 2001, respectively. From 2001 to 2004, she was a postdoctoral fellow in the Department of Electrical and Computer Engineering at the University of Canterbury. In 2002, she spent 5 months as a visiting researcher at the University of Hawaii, USA. Since 2004 she has been working at the University of Canterbury as a lecturer and then as a senior lecturer. Currently, she is an Associate Professor at the same department. In 2007, she was awarded the University of Canterbury, College of Engineering young researcher award. She served as an Editor for the IEEE TRANSACTIONS ON WIRELESS COMMUNICATIONS 2005–2008 and regularly serves on technical program committees for IEEE conferences.

Her current research interests include multilevel coding, error correction coding, iterative decoding and equalization, space-time coding and detection, cognitive radio and cooperative communications in particular for wireless communications.